

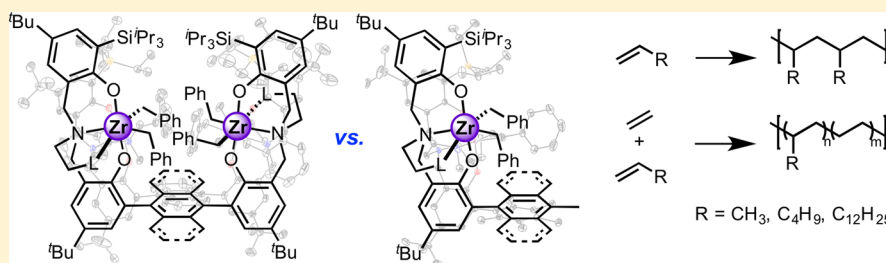
# Olefin Polymerization by Dinuclear Zirconium Catalysts Based on Rigid Teraryl Frameworks: Effects on Tacticity and Copolymerization Behavior

Jessica Sampson,<sup>†</sup> Gyeongshin Choi,<sup>†</sup> Muhammed Naseem Akhtar,<sup>‡</sup> E. A. Jaseer,<sup>‡</sup> Rajesh Theravalappil,<sup>‡</sup> Hassan Ali Al-Muallem,<sup>§</sup> and Theodor Agapie<sup>\*,†</sup>

<sup>†</sup>Division of Chemistry and Chemical Engineering, California Institute of Technology, Pasadena, California 91125, United States

<sup>‡</sup>Center for Refining and Petrochemicals and <sup>§</sup>Department of Chemistry, King Fahd University of Petroleum and Minerals, Dhahran, 31261, Saudi Arabia

## Supporting Information



**ABSTRACT:** Toward gaining insight into the behavior of bimetallic catalysts for olefin polymerization, a series of structurally related binuclear zirconium catalysts with bisamine bisphenolate and pyridine bisphenolate ligands connected by rigid teraryl units were synthesized. Anthracene-9,10-diyl and 2,3,5,6-tetramethylbenzene-1,4-diyl were employed as linkers. Bulky Si<sup>i</sup>Pr<sub>3</sub> and SiPh<sub>3</sub> substituents were used in the position ortho to the phenolate oxygen. Pseudo-C<sub>s</sub> and C<sub>2</sub> symmetric isomers are observed for the binuclear complexes of bisamine bisphenolate ligands. In general, binuclear catalysts show higher isotacticity compared to the monozirconium analogues, with some differences between isomers. Amine bisphenolate-supported dizirconium complexes were found to be moderately active (up to 1.5 kg mmol<sub>Zr</sub><sup>-1</sup> h<sup>-1</sup>) for the polymerization of 1-hexene to isotactically enriched poly-1-hexene (up to 45% *mmmm*) in the presence of stoichiometric trityl or anilinium borate activators. Moderate activity was observed for the production of isotactically enriched polypropylene (up to 2.8 kg mmol<sub>Zr</sub><sup>-1</sup> h<sup>-1</sup> and up to 25.4% *mmmm*). The previously proposed model for tacticity control based on distal steric effects from the second metal site is consistent with the observed behavior. Both bisamine bisphenolate and pyridine bisphenolate supported complexes are active for the production of polyethylene in the presence of MAO with activities in the range of 1.1–1.6 kg mmol<sub>Zr</sub><sup>-1</sup> h<sup>-1</sup> and copolymerize ethylene with  $\alpha$ -olefins. Little difference in the level of  $\alpha$ -olefin incorporation is observed between mono- and dinuclear catalysts supported with the pyridine bisphenolate catalysts. In contrast, the size of the olefin affects the level of incorporation differently between monometallic and bimetallic catalysts for the bisamine bisphenolate system. The ratio of the incorporation levels with dinuclear vs mononuclear catalysts decreases with increasing comonomer size. This effect is attributed to steric pressure provided by the distal metal center on the larger olefin in dinuclear catalysts.

## INTRODUCTION

Dinuclear early and late transition metal catalysts have been studied for improved performance in polyolefin synthesis.<sup>1</sup> Enhanced activity, incorporation of  $\alpha$ -olefins, tolerance to functional groups, and tacticity control are among the benefits demonstrated for dinuclear catalysts compared to related mononuclear catalysts. Enhanced activity and 1-hexene incorporation were reported for dizirconium catalysts supported by dimethylsilyl-linked cyclopentadienyl-amide ligands linked via an alkane-diyl chain (A, Figure 1).<sup>2</sup> Increased 1-hexene incorporation was reported with dizirconium complexes supported by fused phenoxy-imine ligands (B).<sup>3</sup> Pyridine-amide dihafnium complexes with naphthalene-based linkers show enhanced activity for polymerization of ethylene with 1-octene,

higher molecular weights, and increased incorporation of the comonomer (C).<sup>4</sup> Enhanced  $\alpha$ -olefin incorporation by double-decker-type dinickel phenoxy-imine catalysts (D)<sup>5</sup> and enhanced activity for 1-hexene polymerization with enhanced chain straightening by related double-decker  $\alpha$ -diimine dipalladium catalysts have been reported (E).<sup>6</sup> We have reported enhanced incorporation of unprotected amino olefins and enhanced amine tolerance with dinickel phenoxy-imine catalysts linked via *para*- and *meta*-terphenyl moieties (F).<sup>7</sup>

Multinuclear catalysts have also been explored for tacticity control, in particular with early metals, though to a much lesser

Received: January 9, 2017

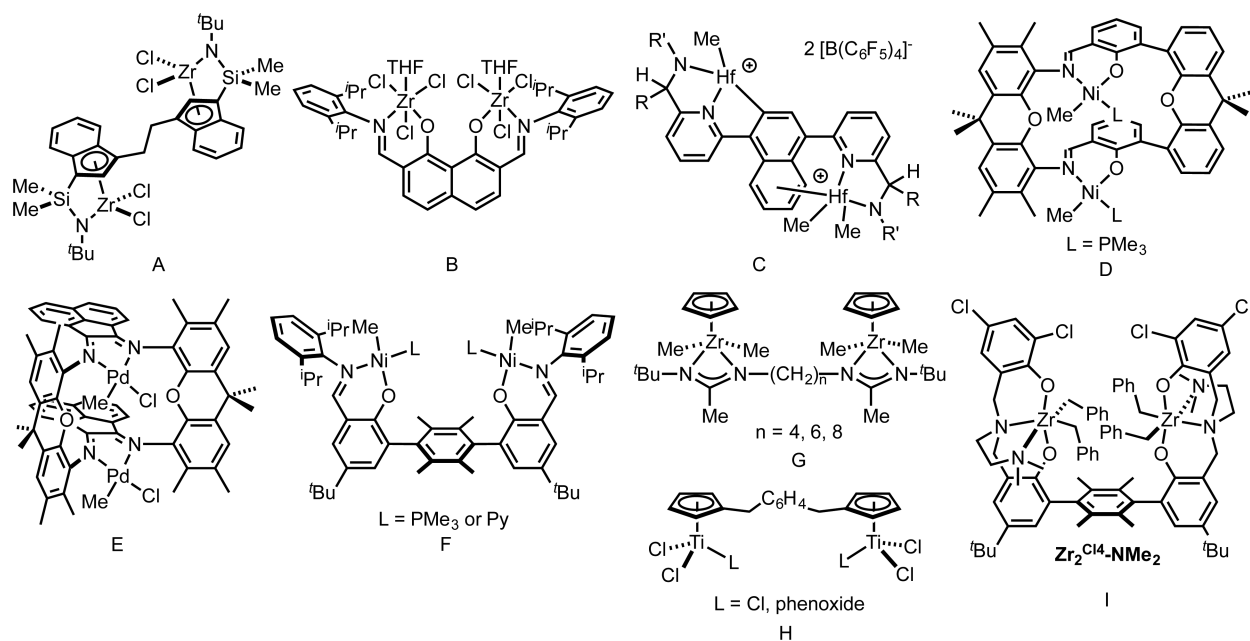


**Figure 1.** Selected example of previously reported dinuclear polymerization catalysts.

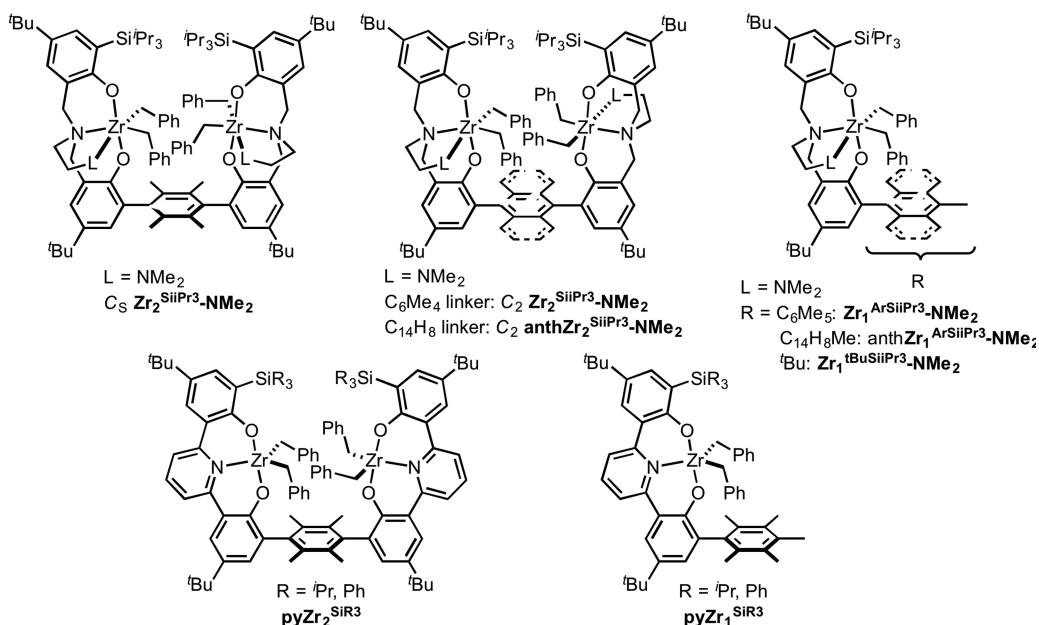


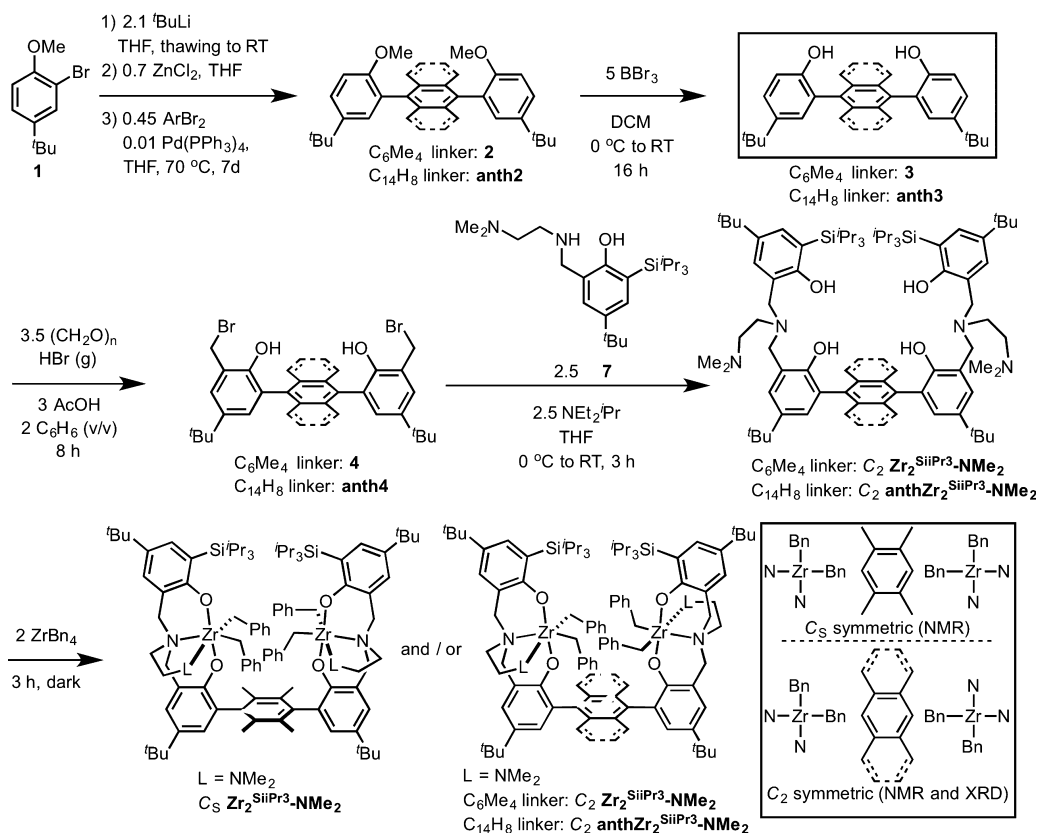
**Figure 2.** Compounds prepared and evaluated in this study.

extent than mononuclear systems.<sup>8,9</sup> Dizirconium bis-propagators supported by amidinate ligands (G) exhibit similar stereoselectivity in the presence of ZnEt<sub>2</sub> to that in its absence, in contrast with monometallic catalysts, which typically exhibit lower selectivity in the presence of the chain transfer reagent.<sup>10</sup> Dinuclear titanocene complexes (H) show enhanced syndiotacticity in styrene polymerization relative to the corresponding monotitanium catalysts.<sup>11</sup>

We have previously reported that bimetallic zirconium amine bisphenolate complexes supported by a rigid *para*-terphenyl linker polymerize propylene and 1-hexene with enhanced activity and tacticity control.<sup>12</sup> Dinuclear Zr<sub>2</sub><sup>Cl<sup>4</sup></sup>-NMe<sub>2</sub> and Zr<sub>2</sub><sup>Cl<sup>4</sup></sup>-OMe have activities of up to 10<sup>3</sup> kg mmol<sub>Zr</sub><sup>-1</sup> h<sup>-1</sup> in 1-hexene polymerization and produce poly-1-hexene with >75% *mmmm*. The greater activities and isoselectivities of these

complexes are attributed to both the ligand environment around each isolated metal center and the interactions of the growing polymer chain with the sterics of the distal metal center. For comparison, the original C<sub>s</sub> symmetric bisamine bisphenolate system reported by Kol and co-workers has activities of up to 10<sup>2</sup> kg mmol<sub>Zr</sub><sup>-1</sup> h<sup>-1</sup> and produces atactic poly-1-hexene.<sup>13</sup> Related C<sub>2</sub> symmetric catalysts produce >95% isotactic poly-1-hexene, but with significantly lower activity, although C<sub>1</sub> symmetric versions show enhanced activity with lower isoselectivity.<sup>14</sup>

Our previous report demonstrated that dizirconium bisamine bisphenolate complexes with bulkier *tert*-butyl substituents were less active and produced poly-1-hexene and polypropylene with lower tacticity control compared to complexes with smaller chloride substituents. A combination of steric effects,

Scheme 1. Preparation of Phenols and Dinuclear Complexes  $Zr_2^{SiPr_3}\text{-NMe}_2$  and  $\text{anth}Zr_2^{SiPr_3}\text{-NMe}_2$  Complexes<sup>a</sup>

<sup>a</sup>Inset: top view of the coordination environment and linker for the C<sub>S</sub> and C<sub>2</sub> isomers.

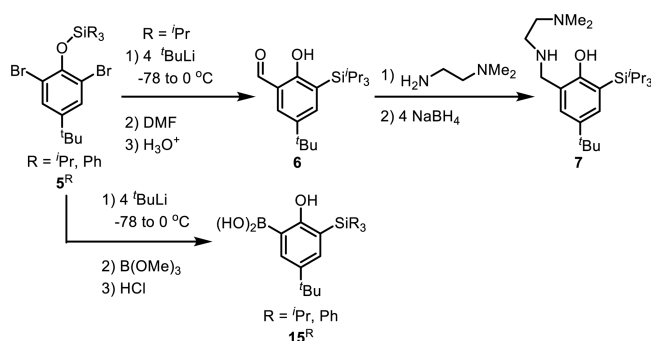
including the distal pressure of the second metal and the difference in size between the small chloride substituent and the large aryl substituent that also serves as linker, was proposed to account for the observed changes in activity and tacticity between mono- and dinuclear catalysts. Variations in the electronic properties of the substituents likely contribute to differences in behavior among the various monometallic or bimetallic catalysts. As options to replace the chloride substituent with a smaller one are very limited, the opposite strategy of significantly increasing the steric bulk is appealing. To gain further insight into structure–function correlations of these dinuclear catalysts, determining the effect of the type of linker employed is desirable. Further related to the steric constraints generated within the coordination sphere of dizirconium complexes, the role of denticity of supporting ligand is of interest. In this context, pyridine bisphenolate systems provide a more open, tridentate ligand framework, to compare to the tetradentate bisamine bisphenolate complexes. Monometallic pyridine bisphenolate complexes have previously been shown to be active catalysts for ethylene and propylene homopolymerization and ethylene– $\alpha$ -olefin copolymerization.<sup>15</sup> Herein we report the synthesis and characterization of the dizirconium bisamine bisphenolate and pyridine bisphenolate complexes (Figure 2) and their ethylene, propylene, 1-hexene, and 1-tetradecene homo- and copolymerization behavior.

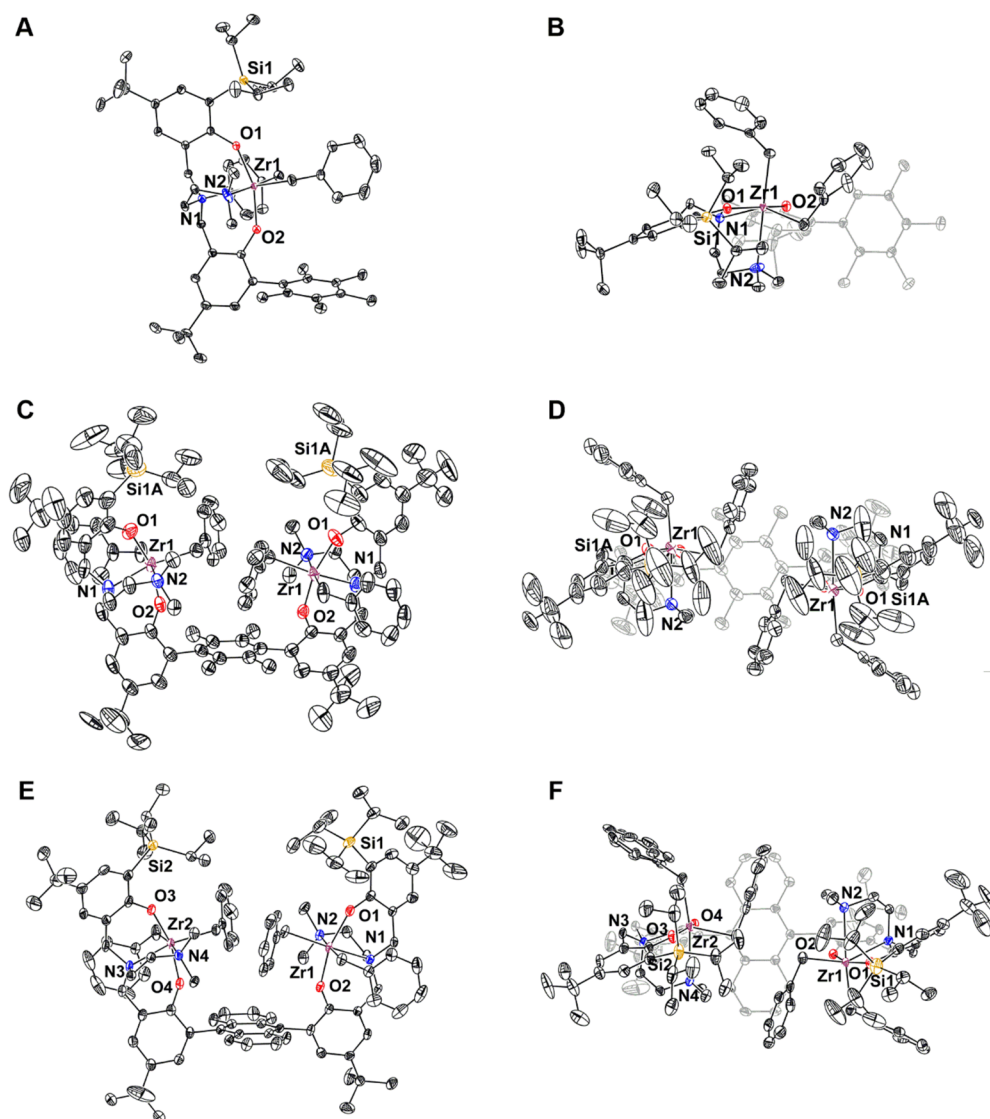
## RESULTS AND DISCUSSION

Dinuclear amine bisphenolate complexes based on a *para*-terphenyl framework were synthesized analogously to the

previously reported catalysts<sup>12</sup> (Scheme 1). Double Negishi coupling of 2-bromo-4-*tert*-butylanisole with 1,4-dibromo-2,3,5,6-tetramethylbenzene or 9,10-dibromoanthracene affords the corresponding terphenyl compounds **2** and **anth-2** with tetramethylphenyl and anthracenyl linkers. Upon removal of protecting groups with boron tribromide, the *syn* and *anti* atropisomers of the resulting phenols (**3** and **anth-3**) were separated by column chromatography. The *syn* atropisomers were further treated with paraformaldehyde and gaseous hydrogen bromide to afford ligand precursors **4** and **anth-4**. Ligand precursor **7** was synthesized starting with the silylation of 2,6-dibromo-4-*tert*-butylphenol (Scheme 2). Subsequent *retro*-Brook rearrangement and quenching with dimethylformamide affords tri-isopropyl-substituted salicylaldehyde **6**. Reductive amination of this species with *N,N*-dimethylethylenediamine

## Scheme 2. Synthesis of Phenol Ligand Precursors Featuring *ortho*-SiR<sub>3</sub> Substituents (R = <sup>t</sup>Pr, Ph)



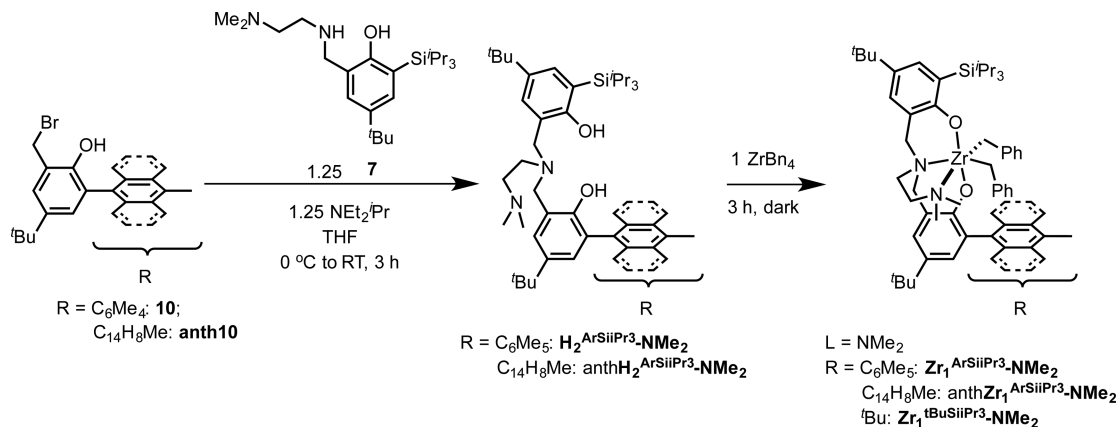
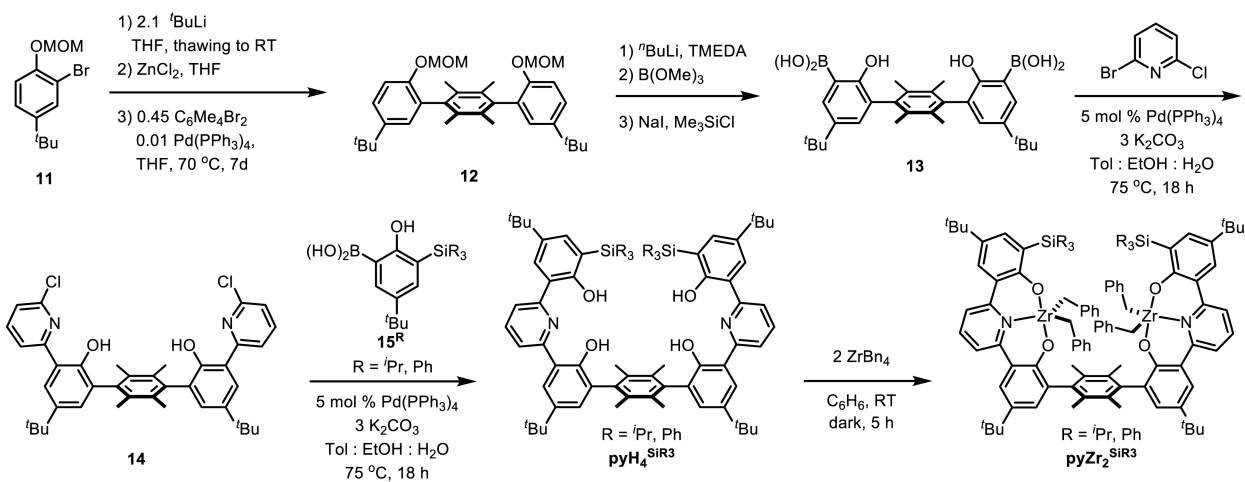


**Figure 3.** Solid-state structures of  $Zr_1^{ArSiPr_3}\text{-NMe}_2$  (top),  $C_2 Zr_2^{SiPr_3}\text{-NMe}_2$  (center), and  $C_2 \text{anthZr}_2^{SiPr_3}\text{-NMe}_2$  (bottom). Views perpendicular to the plane of the linker (D and F) or aryl substituent ortho to phenoxide oxygen (B) are shown on the right. Ellipsoids are drawn at the 50% probability level, and H atoms are omitted for clarity.

amine affords **7**. Reaction of **4** and **anth-4** with **7** in the presence of  $\text{NEt}^i\text{Pr}_2$  produces the desired proligands  $\text{H}_4^{SiPr_3}\text{-NMe}_2$  and  $\text{anth-H}_4^{SiPr_3}\text{-NMe}_2$ , which were purified by column chromatography and isolated in moderate yields ( $\sim 55\%$ ).

Dizirconium complexes supported by these new binucleating ligands were prepared by protonolysis of the phenolic proligands with two equivalents of tetrabenzylzirconium, resulting in a mixture of  $C_s$  and  $C_2$  symmetric metalation isomers. Metalation of  $\text{H}_4^{SiPr_3}\text{-NMe}_2$  affords that mixture in a roughly one to one ratio. Solubility differences between the two isomers allowed isolation of the  $C_s$  complex (in up to 95% purity) and the  $C_2$  complex (analytically pure) following recrystallization, each in roughly 25% overall yield. The structure of  $C_2 Zr_2^{SiPr_3}\text{-NMe}_2$  was confirmed by single-crystal X-ray diffraction (XRD) analysis (Figure 3). The two Zr centers adopt similar geometries to those seen in previously reported mono- and bimetallic complexes with bisamine bisphenolate ligands. The distance between the two metal centers is 7.74 Å, longer by more than 0.1 Å than in the solid-state structure of  $Zr_2^{Cl_4}\text{-NMe}_2$  (7.62 Å), which has the longest distance between

the two metal centers of the previously reported dinuclear complexes linked by terphenyl frameworks. The slightly longer distance between the metal centers may be due to the bulky substituents applying steric pressure on the benzyl ligands. Metalation of  $\text{anthH}_4^{SiPr_3}\text{-NMe}_2$  afforded the  $C_2$  symmetric complex in 85% purity based on  $^1\text{H}$  NMR analysis of the crude reaction mixture. Low-temperature metalation improved this to 95%. Recrystallization of this mixture affords analytically pure  $C_2$  isomer. The identity of the isolated complex was confirmed by XRD (Figure 3). The two Zr centers again adopt similar coordination environments to those in previously reported Zr complexes of bisamine bisphenolate ligands. The overall geometry of the dinuclear species is similar to that of the  $C_2 Zr_2^{SiPr_3}\text{-NMe}_2$  complex. The Zr–Zr distance (7.604 Å) is shorter by more than 0.1 Å compared to the tetramethylphenyl-linked complex. The slightly shorter metal–metal distance may be a consequence of the anthracene linker being flatter than tetramethylbenzene and alleviating some steric constraints in the cavity between the two metal centers. Related *meta*-terphenyl-linked complexes, triphenylsilyl-substituted, and

Scheme 3. Synthesis of Monozirconium Bisamine Bisphenolate Complexes Featuring *ortho*-SiPr<sub>3</sub> SubstituentsScheme 4. Preparation of  $pyZr_2^{SiPr_3}$  and  $pyZr_2^{SiPh_3}$  via Protonolysis of the Corresponding Binucleating Proligands  $pyH_4^{SiPr_3}$  and  $pyH_4^{SiPh_3}$  with Two Equivalents of  $ZrBn_4$ Table 1. 1-Hexene and Propylene Homopolymerizations<sup>a</sup>

entry	catalyst	monomer	activator	yield (g)	activity (kg mmol <sub>Zr</sub> <sup>-1</sup> h <sup>-1</sup> )	% <i>mmmm</i> <sup>b</sup>
1	$Zr_1^{ArSiPr_3-NMe_2}$	1-hexene	$[CPh_3][B(C_6F_5)_4]$	0.076	0.11	34
2	$Zr_1^{ArSiPr_3-NMe_2}$	1-hexene	$[HNMe_2Ph][B(C_6F_5)_4]$	0.046	0.069	37
3	$Zr_1^{ArSiPr_3-NMe_2}$	1-hexene	MAO	0.116	0.17	40
4	$C_5 Zr_2^{SiPr_3-NMe_2}$	1-hexene	$[CPh_3][B(C_6F_5)_4]$	0.067	0.10	45
5	$C_5 Zr_2^{SiPr_3-NMe_2}$	1-hexene	$[HNMe_2Ph][B(C_6F_5)_4]$	0.238	0.36	45
6	$C_5 Zr_2^{SiPr_3-NMe_2}$	1-hexene	MAO	0.613	0.92	10
7	$C_2 Zr_2^{SiPr_3-NMe_2}$	1-hexene	$[CPh_3][B(C_6F_5)_4]$	0.513	0.77	34
8	$C_2 Zr_2^{SiPr_3-NMe_2}$	1-hexene	$[HNMe_2Ph][B(C_6F_5)_4]$	0.596	0.89	34
9	$C_2 Zr_2^{SiPr_3-NMe_2}$	1-hexene	MAO	0.676	1.0	15
10	<b>anth</b> $Zr_1^{ArSiPr_3-NMe_2}$	1-hexene	$[CPh_3][B(C_6F_5)_4]$	0.036	0.054	5
11	<b>anth</b> $Zr_1^{ArSiPr_3-NMe_2}$	1-hexene	$[HNMe_2Ph][B(C_6F_5)_4]$	0.046	0.069	3
12	<b>anth</b> $Zr_1^{ArSiPr_3-NMe_2}$	1-hexene	MAO	0.204	0.31	4
13	$C_2$ <b>anth</b> $Zr_2^{SiPr_3-NMe_2}$	1-hexene	$[CPh_3][B(C_6F_5)_4]$	0.870	1.3	28
14	$C_2$ <b>anth</b> $Zr_2^{SiPr_3-NMe_2}$	1-hexene	$[HNMe_2Ph][B(C_6F_5)_4]$	0.980	1.5	33
15	$C_2$ <b>anth</b> $Zr_2^{SiPr_3-NMe_2}$	1-hexene	MAO	0.860	1.3	42
16	$Zr_1^{ArSiPr_3-NMe_2}$	propylene	MAO	5.5	0.55	14
17	$C_5 Zr_2^{SiPr_3-NMe_2}$	propylene	MAO	19	1.9	19
18	$C_2 Zr_2^{SiPr_3-NMe_2}$	propylene	MAO	22	2.2	25
19	<b>anth</b> $Zr_1^{ArSiPr_3-NMe_2}$	propylene	MAO	9.6	0.96	15
20	$C_2$ <b>anth</b> $Zr_2^{SiPr_3-NMe_2}$	propylene	MAO	28	2.8	24

<sup>a</sup>1-Hexene polymerizations were run with 4.0  $\mu$ mol of Zr, 1 equiv of  $[B(C_6F_5)_4]$  activator or 250 equiv of dried MAO, and 5000 equiv (2.5 mL) of 1-hexene in 2.5 mL of PhCl for 10 min, and propylene polymerizations were run with 10  $\mu$ mol of Zr, 1000 equiv (2.5 mL) of MAO, and 5 bar of propylene in 85 mL of toluene for 60 min in a 250 mL reactor. <sup>b</sup>From integration of the  $^{13}C\{^1H\}$  NMR spectra.

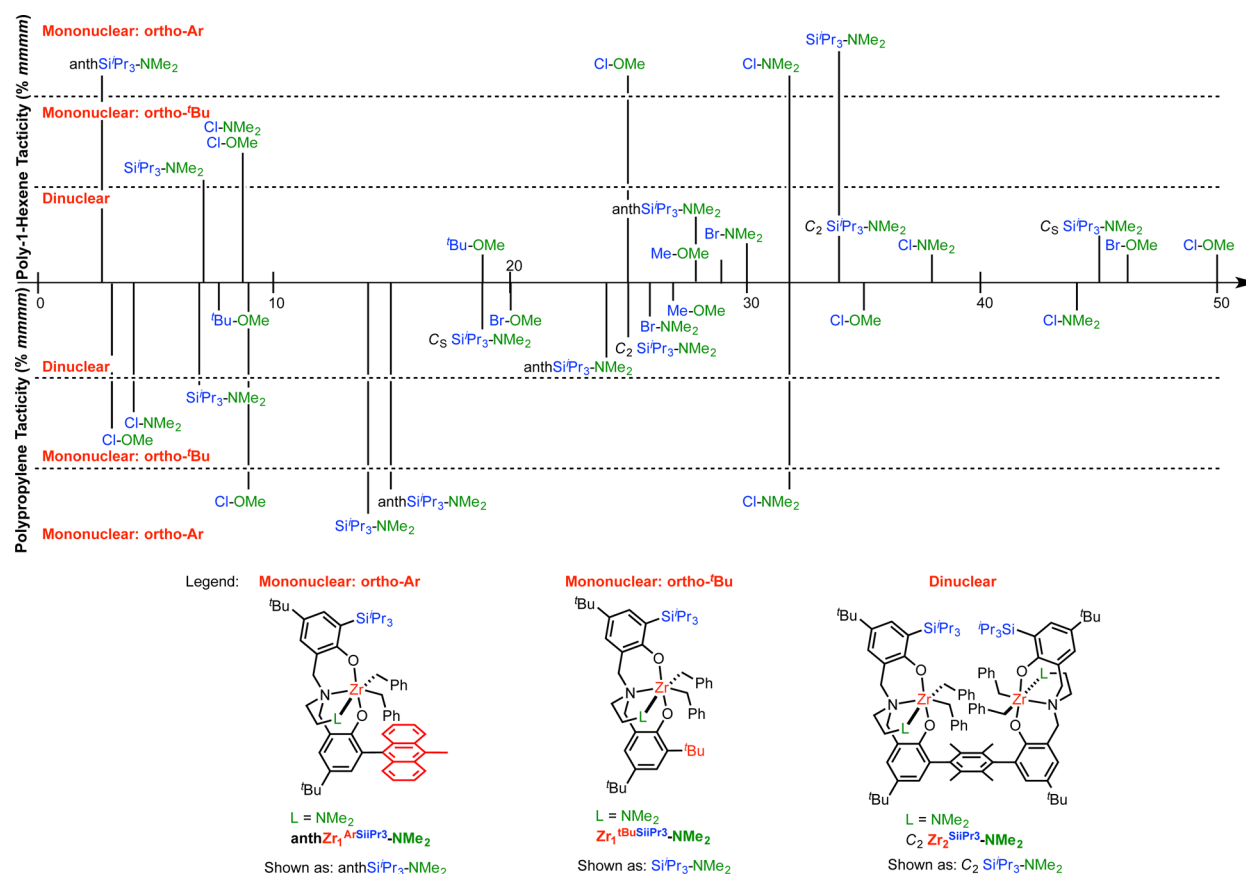


**Figure 4.** Comparison of tacticity control by dinuclear catalysts with substituents ortho to phenoxide oxygens shown in blue and pendant donors, *L*, in green and by monometallic catalysts with either *ortho*-aryl substituents (Ar = C<sub>6</sub>Me<sub>5</sub> or 9-methylanthracenyl) or *ortho-tert*-butyl substituents. 1-Hexene polymerizations were run with [CPh<sub>3</sub>][B(C<sub>6</sub>F<sub>5</sub>)<sub>4</sub>], and propylene polymerizations were run with excess MAO as activators. Legend at bottom provides graphical representations of catalysts and abbreviations under each class of compounds.

Zr<sub>2</sub><sup>SiPr<sub>3</sub></sup>-OMe were also targeted, but single metalation isomers of these complexes could not be isolated. The monometallic complexes Zr<sub>1</sub><sup>Ar</sup>SiPr<sub>3</sub>-NMe<sub>2</sub>, anthZr<sub>1</sub><sup>Ar</sup>SiPr<sub>3</sub>-NMe<sub>2</sub>, and Zr<sub>1</sub><sup>tBu</sup>SiPr<sub>3</sub>-NMe<sub>2</sub> were synthesized by protonolysis of the corresponding proligand with 1 equiv of ZrBn<sub>4</sub> (Scheme 3). The structure of Zr<sub>1</sub><sup>Ar</sup>SiPr<sub>3</sub>-NMe<sub>2</sub> was also confirmed by XRD (Figure 3).

Dizirconium complexes supported by binucleating pyridine bisphenolate ligands were synthesized according to Scheme 4. *Ortho*-lithiation of the *syn* atropisomer of **12** followed by treatment with trimethylborate and subsequent *in situ* deprotection affords boronic acid **13**. Suzuki coupling with 2-bromo-6-chloropyridine provides access to ligand precursor **14**. Species **15<sup>R</sup>** (R = Si<sup>i</sup>Pr<sub>3</sub> and SiPh<sub>3</sub>) were synthesized through *retro*-Brook rearrangement of the corresponding silyl ethers **5<sup>R</sup>** and quenched with trimethylborate (Scheme 2). Suzuki coupling of two equivalents of **15<sup>R</sup>** with **14** affords the final binucleating proligands pyH<sub>4</sub><sup>SiPr<sub>3</sub></sup> and pyH<sub>4</sub><sup>SiPh<sub>3</sub></sup> in moderate overall yields. Mononucleating ligands pyH<sub>2</sub><sup>SiPr<sub>3</sub></sup> and pyH<sub>2</sub><sup>SiPh<sub>3</sub></sup> were synthesized analogously.

Reaction of phenol proligands with two equivalents of ZrBn<sub>4</sub> afforded in quantitative yields single species that display NMR spectroscopic characteristics consistent with the desired products, pyZr<sub>2</sub><sup>SiPr<sub>3</sub></sup> and pyZr<sub>2</sub><sup>SiPh<sub>3</sub></sup>. Only two resonances corresponding to the benzylic CH<sub>2</sub> moiety are observed in the <sup>1</sup>H NMR spectra of pyZr<sub>2</sub><sup>SiPr<sub>3</sub></sup> and pyZr<sub>2</sub><sup>SiPh<sub>3</sub></sup>, indicating that the complexes are C<sub>2v</sub> symmetric on the NMR time scale. Mononuclear Zr dibenzyl complexes were synthesized

analogously and also feature only two CH<sub>2</sub> benzylic resonances, indicating C<sub>s</sub> symmetry on the <sup>1</sup>H NMR time scale.

**1-Hexene and Propylene Homopolymerization.** The precatalyst performance in 1-hexene polymerization was tested under three sets of conditions: upon activation with stoichiometric amounts of [CPh<sub>3</sub>][B(C<sub>6</sub>F<sub>5</sub>)<sub>4</sub>] or [HNMe<sub>2</sub>Ph][B(C<sub>6</sub>F<sub>5</sub>)<sub>4</sub>] and with excess MAO. The bimetallic bisamine bisphenolate complexes show moderate activity and produce isotactically enriched poly-1-hexene in the presence of stoichiometric [CPh<sub>3</sub>][B(C<sub>6</sub>F<sub>5</sub>)<sub>4</sub>] and [HNMe<sub>2</sub>Ph][B(C<sub>6</sub>F<sub>5</sub>)<sub>4</sub>] activators. C<sub>2</sub>Zr<sub>2</sub><sup>SiPr<sub>3</sub></sup>-NMe<sub>2</sub> and C<sub>2</sub>anthZr<sub>2</sub><sup>SiPr<sub>3</sub></sup>-NMe<sub>2</sub> generate poly-1-hexene with ca. 30% *mmmm* content with activities in the range of 0.77–1.5 kg mmol<sub>Zr</sub><sup>-1</sup> h<sup>-1</sup> (Table 1, entries 7, 8, 13, and 14). In the presence of MAO as a cocatalyst the activity of both C<sub>2</sub> and C<sub>s</sub> Zr<sub>2</sub><sup>SiPr<sub>3</sub></sup>-NMe<sub>2</sub> is improved, but the tacticity control is lowered to only 10 and 15% *mmmm*, respectively (Table 1, entries 6 and 9). C<sub>s</sub>Zr<sub>2</sub><sup>SiPr<sub>3</sub></sup>-NMe<sub>2</sub> has improved tacticity control, producing poly-1-hexene with 45% *mmmm* content in the presence of [CPh<sub>3</sub>][B(C<sub>6</sub>F<sub>5</sub>)<sub>4</sub>] and [HNMe<sub>2</sub>Ph][B(C<sub>6</sub>F<sub>5</sub>)<sub>4</sub>] (Table 1, entries 4 and 5). In contrast, C<sub>2</sub>Zr<sub>2</sub><sup>SiPr<sub>3</sub></sup>-NMe<sub>2</sub> has overall lower isotacticity (34% *mmmm*) for 1-hexene homopolymerization in the presence of the borate counteranion as compared to the C<sub>s</sub> isomer, although with improved activity (Table 1, entries 4 and 5 vs 7 and 8). All dinuclear catalysts show a slight improvement in activity in the presence of [HNMe<sub>2</sub>Ph][B(C<sub>6</sub>F<sub>5</sub>)<sub>4</sub>] compared to [CPh<sub>3</sub>][B(C<sub>6</sub>F<sub>5</sub>)<sub>4</sub>]. Monometallic Zr<sub>1</sub><sup>Ar</sup>SiPr<sub>3</sub>-NMe<sub>2</sub> shows lower activities and similar tacticities to the dinuclear catalysts, except in the

Table 2. Ethylene Homopolymerizations and Ethylene–Propylene Copolymerizations<sup>a</sup>

	catalyst	% C <sub>2</sub> feed	% C <sub>3</sub> feed	yield (g)	activity (kg mmol <sub>Zr</sub> <sup>-1</sup> h <sup>-1</sup> )	M <sub>N</sub> (kDa)	PDI <sup>b</sup>	T <sub>M</sub> (°C)	% I <sup>c</sup> (C <sub>3</sub> )
1	Zr <sub>1</sub> <sup>ArSiPr<sub>3</sub></sup> -NMe <sub>2</sub>	100	0	16	1.6	4.7	47	133	
2	C <sub>s</sub> Zr <sub>2</sub> <sup>SiPr<sub>3</sub></sup> -NMe <sub>2</sub>	100	0	11	1.1	17	23	134	
3	C <sub>2</sub> Zr <sub>2</sub> <sup>SiPr<sub>3</sub></sup> -NMe <sub>2</sub>	100	0	14	1.4	27	29	133	
4	anthZr <sub>1</sub> <sup>SiPr<sub>3</sub></sup> -NMe <sub>2</sub>	100	0	15	1.5	8.6	15	132	
5	C <sub>2</sub> anthZr <sub>2</sub> <sup>SiPr<sub>3</sub></sup> -NMe <sub>2</sub>	100	0	14	1.4	21	32	134	
6	pyZr <sub>1</sub> <sup>ArSiPr<sub>3</sub></sup>	100	0	14	1.4	9.9	40	135	
7	pyZr <sub>2</sub> <sup>SiPr<sub>3</sub></sup>	100	0	12	1.2	4.6	30	133	
8	pyZr <sub>1</sub> <sup>ArSiPh<sub>3</sub></sup>	100	0	13	1.3	4.9	34	132	
9	pyZr <sub>2</sub> <sup>SiPh<sub>3</sub></sup>	100	0	12	1.2	4.7	44	132	
10	Zr <sub>1</sub> <sup>ArSiPr<sub>3</sub></sup> -NMe <sub>2</sub>	25	75	15	1.5	3.6	6.0	76	25
11	C <sub>s</sub> Zr <sub>2</sub> <sup>SiPr<sub>3</sub></sup> -NMe <sub>2</sub>	25	75	21	2.1	12	6.6	108	52
12	C <sub>2</sub> Zr <sub>2</sub> <sup>SiPr<sub>3</sub></sup> -NMe <sub>2</sub>	25	75	20	2.0	11	6.7	111	40
13	anthZr <sub>1</sub> <sup>SiPr<sub>3</sub></sup> -NMe <sub>2</sub>	25	75	24	2.4	7.8	4.6	<sup>e</sup>	36
14	C <sub>2</sub> anthZr <sub>2</sub> <sup>SiPr<sub>3</sub></sup> -NMe <sub>2</sub>	25	75	24	2.4	12	6.3	110	49
15	pyZr <sub>1</sub> <sup>ArSiPr<sub>3</sub></sup>	25	75	4.8	0.48	15	10	118	12
16	pyZr <sub>2</sub> <sup>SiPr<sub>3</sub></sup>	25	75	7.2	0.72	5.1	28	117	8
17	pyZr <sub>1</sub> <sup>ArSiPh<sub>3</sub></sup>	25	75	10	1.0	5.3	23	115	9
18	pyZr <sub>2</sub> <sup>SiPh<sub>3</sub></sup>	25	75	6.4	0.64	8.5	13	110	14

<sup>a</sup>Polymerizations were run with 10 μmol of Zr in 85 mL of toluene in the presence of 1000 equiv (2.5 mL) of MAO and 5 bar of ethylene at 60 °C.

<sup>b</sup>PDI determined from GPC measurements, where PDI is defined as M<sub>w</sub>/M<sub>n</sub>. <sup>c</sup>Calculated from DSC measurements. <sup>d</sup>Percentage incorporation of propylene from <sup>13</sup>C{<sup>1</sup>H} NMR integration. <sup>e</sup>Not measured.

presence of the MAO cocatalyst, where the monometallic catalyst shows higher tacticity control. Comparing anthZr<sub>1</sub><sup>ArSiPr<sub>3</sub></sup>-NMe<sub>2</sub> and anthZr<sub>2</sub><sup>SiPr<sub>3</sub></sup>-NMe<sub>2</sub> for 1-hexene polymerization, the dinuclear precatalyst shows significantly greater tacticity control (between 28% and 42% *mmmm* vs between 3% and 5% *mmmm* for anthZr<sub>1</sub><sup>ArSiPr<sub>3</sub></sup>-NMe<sub>2</sub>). C<sub>2</sub> anthZr<sub>2</sub><sup>SiPr<sub>3</sub></sup>-NMe<sub>2</sub> has similar activity and isotacticity compared to C<sub>2</sub> Zr<sub>2</sub><sup>SiPr<sub>3</sub></sup>-NMe<sub>2</sub> in the presence of the stoichiometric activators.

Zr<sub>2</sub><sup>SiPr<sub>3</sub></sup>-NMe<sub>2</sub> and anthZr<sub>2</sub><sup>SiPr<sub>3</sub></sup>-NMe<sub>2</sub> both show moderate activity (1.9–2.8 kg mmol<sub>Zr</sub><sup>-1</sup> h<sup>-1</sup>) for propylene polymerization at 60 °C in toluene in the presence of excess MAO at 5 bar propylene pressure (Table 1, entries 17, 18, and 20). These catalysts produce low-tacticity polypropylene. C<sub>s</sub> Zr<sub>2</sub><sup>SiPr<sub>3</sub></sup>-NMe<sub>2</sub> shows slightly lower tacticity control with 19% *mmmm* as compared to 25% and 24% for C<sub>2</sub> Zr<sub>2</sub><sup>SiPr<sub>3</sub></sup>-NMe<sub>2</sub> and anthZr<sub>2</sub><sup>SiPr<sub>3</sub></sup>-NMe<sub>2</sub> (Table 1, entries 17, 18, and 20). Both Zr<sub>1</sub><sup>ArSiPr<sub>3</sub></sup>-NMe<sub>2</sub> and anthZr<sub>1</sub><sup>ArSiPr<sub>3</sub></sup>-NMe<sub>2</sub> have lower activity (0.55 and 0.96 kg mmol<sub>Zr</sub><sup>-1</sup> h<sup>-1</sup>, respectively) than the dinuclear catalysts and show lower tacticity control (ca. 14% *mmmm*) (Table 1, entries 16 and 19).

Generally, the mononuclear catalysts show significantly lower activity and tacticity control compared to the dinuclear analogues. These differences may be explained in terms of the distal steric effect of the second metal, limiting anion association and degrees of freedom for olefin insertion.<sup>12</sup> The observed differences between the C<sub>2</sub> and C<sub>s</sub> Zr<sub>2</sub><sup>SiPr<sub>3</sub></sup>-NMe<sub>2</sub> isomers suggest that the particular coordination environment of the distal metal center affects reactivity, despite being remote. The shape of the cavity between the two metal centers has consequences on both tacticity and activity.

In comparison with the previously reported complexes bearing *ortho*-pentamethylphenyl substituents, Zr<sub>1</sub><sup>ArSiPr<sub>3</sub></sup>-NMe<sub>2</sub> shows a decrease in activity relative to Zr<sub>1</sub><sup>ArCl<sub>2</sub></sup>-NMe<sub>2</sub> (1.5–1.9 kg mmol<sub>Zr</sub><sup>-1</sup> h<sup>-1</sup>) with fairly similar tacticity control in 1-hexene polymerization (24–25% *mmmm* for Zr<sub>1</sub><sup>ArCl<sub>2</sub></sup>-NMe<sub>2</sub> and 31–32% *mmmm* for Zr<sub>1</sub><sup>ArSiPr<sub>3</sub></sup>-NMe<sub>2</sub>, Figure 4).<sup>12</sup> anthZr<sub>1</sub><sup>ArSiPr<sub>3</sub></sup>-NMe<sub>2</sub> shows significantly lower tacticity control as compared to these catalysts. For propylene polymerization upon activation

with MAO, however, Zr<sub>1</sub><sup>ArSiPr<sub>3</sub></sup>-NMe<sub>2</sub> and anthZr<sub>1</sub><sup>ArSiPr<sub>3</sub></sup>-NMe<sub>2</sub> show similar tacticity control, both lower than Zr<sub>1</sub><sup>ArCl<sub>2</sub></sup>-NMe<sub>2</sub>. The <sup>t</sup>Bu-substituted catalysts generally show very low tacticity control. The lower activity of the new catalysts is consistent with the previous observation of higher 1-hexene polymerization activities from complexes bearing ligands with electron-withdrawing substituents.<sup>12,21</sup> The lack of significant improvements in tacticity control for Zr<sub>1</sub><sup>ArSiPr<sub>3</sub></sup>-NMe<sub>2</sub> and anthZr<sub>1</sub><sup>ArSiPr<sub>3</sub></sup>-NMe<sub>2</sub> could result from one or several features of the previously proposed mechanism, including site epimerization and selectivity of monomer insertion based on steric control of polymer orientation by the bulk of the aryl substituent. With the more bulky Si<sup>i</sup>Pr<sub>3</sub> substituents, the difference between the two phenolates is less pronounced, potentially leading to less control of polymer chain orientation. The more spherical <sup>t</sup>Bu substituent does not provide efficient tacticity control likely because it is less expansive compared to the pentamethylphenyl and anthracenyl substituents.

In comparison with the previously reported bimetallic catalysts supported by amine bisphenolate ligands bearing the bulky *ortho-tert*-butyl substituent (Zr<sub>2</sub><sup>tBu<sub>2</sub></sup>-OMe), the new C<sub>2</sub> symmetric complexes have similar activities for 1-hexene polymerization (~1 kg mmol<sub>Zr</sub><sup>-1</sup> h<sup>-1</sup>) but produce significantly more isotactic poly-1-hexene in the presence of the stoichiometric activators (19% *mmmm* for Zr<sub>2</sub><sup>tBu<sub>2</sub></sup>-OMe, Figure 4). C<sub>2</sub> anthZr<sub>2</sub><sup>SiPr<sub>3</sub></sup>-NMe<sub>2</sub> shows similar tacticity control (28% *mmmm*) to the previously reported C<sub>s</sub> and C<sub>2</sub> Zr<sub>2</sub><sup>Me<sub>4</sub></sup>-OMe and to C<sub>2</sub> Zr<sub>2</sub><sup>Br<sub>4</sub></sup>-NMe<sub>2</sub> (28–30% *mmmm*). C<sub>2</sub> and C<sub>s</sub> Zr<sub>2</sub><sup>SiPr<sub>3</sub></sup>-NMe<sub>2</sub> produce similarly isotactically enriched polymer (34% and 45% *mmmm*) to that seen for the more sterically open Zr<sub>2</sub><sup>Cl<sub>4</sub></sup>-NMe<sub>2</sub>, Zr<sub>2</sub><sup>Cl<sub>4</sub></sup>-OMe, and Zr<sub>2</sub><sup>Br<sub>4</sub></sup>-OMe catalysts at room temperature (35% to 50% *mmmm*), albeit with lower activity. Both C<sub>2</sub> anthZr<sub>2</sub><sup>SiPr<sub>3</sub></sup>-NMe<sub>2</sub> and C<sub>2</sub> Zr<sub>2</sub><sup>SiPr<sub>3</sub></sup>-NMe<sub>2</sub> have similar activity for propylene homopolymerization to C<sub>2</sub> Zr<sub>2</sub><sup>tBu<sub>2</sub></sup>-OMe (ca. 2 kg mmol<sub>Zr</sub><sup>-1</sup> h<sup>-1</sup>) but with improved tacticity control (24–25% *mmmm* vs 6–8% *mmmm*). The new complexes with Si<sup>i</sup>Pr<sub>3</sub> substituents show similar tacticity control in propylene polymerization to Zr<sub>2</sub><sup>Br<sub>4</sub></sup>-OMe, Zr<sub>2</sub><sup>Br<sub>4</sub></sup>-NMe<sub>2</sub>, and Zr<sub>2</sub><sup>Me<sub>4</sub></sup>-OMe.

Table 3. Copolymerizations of Ethylene with 1-Hexene and 1-Tetradecene<sup>a</sup>

	catalyst	comonomer	yield (g)	activity (kg mmol <sub>Zr</sub> <sup>-1</sup> h <sup>-1</sup> )	M <sub>n</sub> (kDa)	PDI <sup>b</sup>	T <sub>M</sub> (°C)	% I <sup>c</sup>
1	Zr <sub>1</sub> <sup>ArSiPr<sub>3</sub></sup> -NMe <sub>2</sub>	1-hexene	15	1.5	2.2	3.6	104	19
2	C <sub>s</sub> Zr <sub>2</sub> <sup>SiPr<sub>3</sub></sup> -NMe <sub>2</sub>	1-hexene	19	1.9	5.9	3.7	99	12
3	C <sub>2</sub> Zr <sub>2</sub> <sup>SiPr<sub>3</sub></sup> -NMe <sub>2</sub>	1-hexene	20	2.0	8.8	12	105	22
4	anthZr <sub>1</sub> <sup>SiPr<sub>3</sub></sup> -NMe <sub>2</sub>	1-hexene	24	2.4	7.1	3.4	<sup>g</sup>	28
5	C <sub>2</sub> anthZr <sub>2</sub> <sup>SiPr<sub>3</sub></sup> -NMe <sub>2</sub>	1-hexene	19	1.9	11	8.8	104	30
6	pyZr <sub>1</sub> <sup>ArSiPr<sub>3</sub></sup>	1-hexene	20	2.0	1.6	7.2	115	7
7	pyZr <sub>2</sub> <sup>SiPr<sub>3</sub></sup>	1-hexene	14	1.4	3.5	19	125	4
8	pyZr <sub>1</sub> <sup>ArSiPh<sub>3</sub></sup>	1-hexene	29	2.9	0.8	11	112	7
9	pyZr <sub>2</sub> <sup>SiPh<sub>3</sub></sup>	1-hexene	19	1.9	1.9	35	121	5
10	Zr <sub>1</sub> <sup>ArSiPr<sub>3</sub></sup> -NMe <sub>2</sub>	1-tetradecene	9.7	0.97	17	8.8	61	7
11	C <sub>s</sub> Zr <sub>2</sub> <sup>SiPr<sub>3</sub></sup> -NMe <sub>2</sub>	1-tetradecene	20	2.0	41	<sup>g</sup>	<sup>g</sup>	6
12	C <sub>2</sub> Zr <sub>2</sub> <sup>SiPr<sub>3</sub></sup> -NMe <sub>2</sub>	1-tetradecene	20	2.0	39	26	104	3
13	anthZr <sub>1</sub> <sup>SiPr<sub>3</sub></sup> -NMe <sub>2</sub>	1-tetradecene	25	2.5	12	2.7	110	10
14	C <sub>2</sub> anthZr <sub>2</sub> <sup>SiPr<sub>3</sub></sup> -NMe <sub>2</sub>	1-tetradecene	23	2.3	22	6.6	105	7

<sup>a</sup>Polymerizations were run with 10 μmol of Zr in 65 mL of toluene in the presence of 1000 equiv (2.5 mL) of MAO and 3 bar of ethylene and 20 mL (1.6 × 10<sup>4</sup> equiv) of 1-hexene or 20 mL (7900 equiv) of 1-tetradecene at 60 °C. <sup>b</sup>Yield in g. <sup>c</sup>Activity reported in kg mmol<sub>Zr</sub><sup>-1</sup> h<sup>-1</sup>. <sup>d</sup>M<sub>n</sub> and PDI determined from GPC measurements, where M<sub>n</sub> is reported in kDa and PDI is defined as M<sub>w</sub>/M<sub>n</sub>. <sup>e</sup>Reported in °C, from DSC measurements. <sup>f</sup>% incorporation of the comonomer determined from <sup>13</sup>C{<sup>1</sup>H} NMR integration. <sup>g</sup>Not measured.

Importantly, an extensive set of dinuclear catalysts was compared to mononuclear versions, and in *all* cases, the dinuclear catalysts show improvement in tacticity control (Figure 4). This suggests that the steric pressure provided by the coordination environment of the second metal restricts the orientation of the polymeryl chain and incoming olefin better than that possible in analogous mononuclear systems. Overall, within the series of dinuclear catalysts, increasing steric bulk ortho to the phenolate oxygen away from the linker does not benefit control of tacticity. The smallest substituent, chloride, displays the highest degree of tacticity control. This behavior is consistent with the highest *mmmm* content resulting from maximizing the difference in steric profile relative to the linker, with the smaller chloride substituents ortho to the phenolate oxygen having the largest impact. The much larger silyl substituents likely make the two phenolate sides more similar and less discriminating with respect to interaction with the polymeryl chain and the incoming monomer and, therefore, decrease tacticity control.

**Ethylene Homopolymerization and Ethylene- $\alpha$ -Olefin Copolymerization.** The ethylene homopolymerization of all complexes was investigated in the presence of excess MAO (Table 2). Initial optimization with monometallic Zr<sub>1</sub><sup>tBuSiPr<sub>3</sub></sup>-NMe<sub>2</sub> indicated that addition of AlMe<sub>3</sub> resulted in loss of activity. Improved yield was obtained at 60 °C in the presence of MAO alone (Supporting Information Table S1). Under optimized conditions pyZr<sub>1</sub><sup>ArSiPr<sub>3</sub></sup>, pyZr<sub>2</sub><sup>SiPr<sub>3</sub></sup>, pyZr<sub>1</sub><sup>ArSiPh<sub>3</sub></sup>, and pyZr<sub>2</sub><sup>SiPh<sub>3</sub></sup> all show moderate activity for polyethylene formation (1.2–1.4 kg mmol<sub>Zr</sub><sup>-1</sup> h<sup>-1</sup>) and produce polymers with similar M<sub>n</sub> and PDI values (between 4.7 and 9.9 kDa for M<sub>N</sub> and 30.9 and 44.4 for the PDI values) (Table 2, entries 6–9). Zr<sub>1</sub><sup>ArSiPr<sub>3</sub></sup>-NMe<sub>2</sub> and anthZr<sub>1</sub><sup>ArSiPr<sub>3</sub></sup>-NMe<sub>2</sub> both have slightly improved activities (1.6 and 1.5 kg mmol<sub>Zr</sub><sup>-1</sup> h<sup>-1</sup>, respectively) (Table 2, entries 1 and 4) although not very different from Zr<sub>2</sub><sup>SiPr<sub>3</sub></sup>-NMe<sub>2</sub> and anthZr<sub>2</sub><sup>SiPr<sub>3</sub></sup>-NMe<sub>2</sub> (1.1–1.4 kg mmol<sub>Zr</sub><sup>-1</sup> h<sup>-1</sup>) (Table 2, entries 2, 3, and 5). Under these conditions, although high PDIs (between 15 and 47, with multimodal distributions in some instances) were observed for all catalysts, the M<sub>N</sub> values were higher for the bimetallic catalysts (between 17.2 and 26.7 kDa) as compared with the monometallic catalysts (between

4.7 and 8.6 kDa). The high T<sub>M</sub> values support the formation of linear polymers under these conditions with all catalysts.<sup>22</sup>

Ethylene–propylene copolymerization behavior was tested in the presence of excess MAO under 5 bar total pressure with a 1:3 C<sub>2</sub>:C<sub>3</sub> flow ratio (Table 2). Initial optimization with Zr<sub>1</sub><sup>tBuSiPr<sub>3</sub></sup>-NMe<sub>2</sub> indicated that under these conditions propylene was incorporated well with relatively high overall activity (Supporting Information Table S1). Under these conditions pyZr<sub>1</sub><sup>ArSiPr<sub>3</sub></sup>, pyZr<sub>2</sub><sup>SiPr<sub>3</sub></sup>, pyZr<sub>1</sub><sup>ArSiPh<sub>3</sub></sup>, and pyZr<sub>2</sub><sup>SiPh<sub>3</sub></sup> have lower activities than for ethylene homopolymerization (0.48–1.0 kg mmol<sub>Zr</sub><sup>-1</sup> h<sup>-1</sup>, Table 2, entries 15–18). Both pyZr<sub>2</sub> and pyZr<sub>1</sub> catalysts incorporate low levels of propylene, and while pyZr<sub>2</sub><sup>SiPh<sub>3</sub></sup> shows a slight enhancement in comonomer incorporation over pyZr<sub>1</sub><sup>SiPh<sub>3</sub></sup> (14% C<sub>3</sub> vs 9% C<sub>3</sub>) (Table 2, entries 18 vs 17), pyZr<sub>2</sub><sup>SiPr<sub>3</sub></sup> and pyZr<sub>1</sub><sup>SiPr<sub>3</sub></sup> are very similar (8% C<sub>3</sub> vs 9% C<sub>3</sub>) (Table 2, entries 16 vs 15). The low levels of comonomer incorporation lead to relatively high melting temperatures (110–119 °C). Similar M<sub>n</sub> and PDI values were observed between the catalysts.

Zr<sub>2</sub><sup>SiPr<sub>3</sub></sup>-NMe<sub>2</sub> and C<sub>2</sub> anthZr<sub>2</sub><sup>SiPr<sub>3</sub></sup>-NMe<sub>2</sub> more effectively incorporate propylene than the corresponding monometallic complexes under these conditions. While Zr<sub>1</sub><sup>ArSiPr<sub>3</sub></sup>-NMe<sub>2</sub> incorporates only 25% propylene, C<sub>s</sub> and C<sub>2</sub> Zr<sub>2</sub><sup>SiPr<sub>3</sub></sup>-NMe<sub>2</sub> incorporate 52% and 40%, respectively, and show slightly enhanced activity (2.1 and 2.0 kg mmol<sub>Zr</sub><sup>-1</sup> h<sup>-1</sup>, respectively, vs 1.5 kg mmol<sub>Zr</sub><sup>-1</sup> h<sup>-1</sup> for Zr<sub>1</sub><sup>ArSiPr<sub>3</sub></sup>-NMe<sub>2</sub>) (Table 2, entries 10–12). Similarly, anthZr<sub>1</sub><sup>ArSiPr<sub>3</sub></sup>-NMe<sub>2</sub> incorporates 36% propylene, while anthZr<sub>2</sub><sup>SiPr<sub>3</sub></sup>-NMe<sub>2</sub> incorporates 49% propylene (Table 2, entries 13, 14). Both anthracene-substituted complexes show enhanced activity and propylene incorporation compared with the phenyl-substituted complexes (36% C<sub>3</sub> for anthZr<sub>1</sub><sup>SiPr<sub>3</sub></sup>-NMe<sub>2</sub> vs 25% C<sub>3</sub> for Zr<sub>1</sub><sup>SiPr<sub>3</sub></sup>-NMe<sub>2</sub> (Table 2, entry 13 vs entry 10) and 49% C<sub>3</sub> for C<sub>2</sub> anthZr<sub>2</sub><sup>SiPr<sub>3</sub></sup>-NMe<sub>2</sub> vs 40% C<sub>3</sub> for C<sub>2</sub> Zr<sub>2</sub><sup>SiPr<sub>3</sub></sup>-NMe<sub>2</sub> (Table 2, entry 14 vs entry 12)). In the presence of propylene, lower PDI values were observed for these bisamine bisphenolate complexes (between 4.6 and 6.7), and the M<sub>N</sub> values were higher for the bimetallic catalysts (between 10.6 and 12.2 kDa for the bimetallics and between 3.6 and 7.8 kDa for the monometallics), although the effect is less dramatic than in the ethylene homopolymerizations.

Ethylene–1-hexene copolymerization was investigated in the presence of excess MAO, 3 bar of ethylene, and  $1.6 \times 10^4$  equiv of 1-hexene.  $\text{pyZr}_1^{\text{ArSiPr}_3}$ ,  $\text{pyZr}_2^{\text{SiPr}_3}$ ,  $\text{pyZr}_1^{\text{ArSiPh}_3}$ , and  $\text{pyZr}_2^{\text{SiPh}_3}$  are more active under these conditions than in the presence of propylene as a comonomer or under ethylene homopolymerization conditions, although incorporation of the comonomer is overall low. On the basis of the  $^{13}\text{C}$  NMR spectra of the resulting polymers (Supporting Information, Figures S24 and S25), both  $\text{pyZr}_1^{\text{SiPr}_3}$  and  $\text{pyZr}_1^{\text{SiPh}_3}$  randomly incorporate ca. 7% 1-hexene (Table 3, entries 6 and 8), while  $\text{pyZr}_2^{\text{SiPr}_3}$  and  $\text{pyZr}_2^{\text{SiPh}_3}$  randomly incorporate only 4–5% (Table 3, entries 7 and 9). The resulting polymers have fairly high melting temperatures, consistent with the low, random incorporation.

The monometallic catalysts  $\text{Zr}_1^{\text{ArSiPr}_3}\text{-NMe}_2$  and  $\text{anthZr}_1^{\text{SiPr}_3}\text{-NMe}_2$  both incorporate 1-hexene well (19% and 28%, respectively) with similar activity as in the presence of the propylene comonomer (Table 3, entries 1 and 4). While the  $\text{C}_2$  symmetric  $\text{Zr}_2^{\text{SiPr}_3}\text{-NMe}_2$  and  $\text{anthZr}_2^{\text{SiPr}_3}\text{-NMe}_2$  show modest increases (to 22% and 30%, Table 3, entries 3 and 5) in comonomer incorporation relative to the monometallic analogues,  $\text{C}_s$   $\text{Zr}_2^{\text{SiPr}_3}\text{-NMe}_2$  incorporates less of this comonomer than either the  $\text{C}_2$  dizirconium complexes or the monozirconium complexes (12% 1-hexene incorporation, Table 3, entry 2). PDI values for these catalysts are large under these conditions, with the  $M_n$  values for the polymers obtained from the bimetallic catalysts generally higher compared with the  $M_n$  values from the monometallic catalysts.

To evaluate the effect of comonomer size on incorporation level between mono- and dinuclear catalysts, ethylene–1-tetradecene copolymerizations were also performed using the bisamine bisphenolate catalysts in the presence of MAO, 3 bar of ethylene, and 7900 equiv of 1-tetradecene.  $\text{Zr}_1^{\text{ArSiPr}_3}\text{-NMe}_2$  has lower activity under these conditions than in the presence of propylene or 1-hexene comonomers and incorporates 1-tetradecene at the 7% level (Table 3, entry 10). Both  $\text{C}_s$  and  $\text{C}_2$   $\text{Zr}_2^{\text{SiPr}_3}\text{-NMe}_2$  have similar activities under these conditions, although the incorporation of the comonomer is lower with the dinuclear catalysts than with the mononuclear catalysts (ca. 6% for  $\text{C}_s$   $\text{Zr}_2^{\text{SiPr}_3}\text{-NMe}_2$  and ca. 3% for  $\text{C}_2$   $\text{Zr}_2^{\text{SiPr}_3}\text{-NMe}_2$ ). Similarly,  $\text{anthZr}_2^{\text{SiPr}_3}\text{-NMe}_2$  incorporates around 7% of 1-tetradecene (Table 3, entries 11 and 12), while  $\text{anthZr}_1^{\text{ArSiPr}_3}\text{-NMe}_2$  incorporates more (9%, Table 3, entry 13). Again, higher  $M_n$  values are obtained with the bimetallic catalysts as compared to the monometallic, although the PDI values remain fairly high for all catalysts under these conditions.

The lack of substantial difference in activity between the mono- and dizirconium catalysts supported by pyridine bisphenolate ligands likely results from the more open coordination environment afforded by the tridentate ligand environment. As the metal centers have an additional coordination site available for polymeryl or olefin coordination compared to the bisamine bisphenolate systems, the distal steric effect of the second metal is not consequential. Association of the anion(s) may be relatively facile, leading to attenuation of activity. The lower activity and  $\alpha$ -olefin incorporation may also be related to differences in ligand denticity.<sup>13c,d</sup>

Both  $\text{C}_2$   $\text{anthZr}_2^{\text{SiPr}_3}\text{-NMe}_2$  and  $\text{anthZr}_1^{\text{SiPr}_3}\text{-NMe}_2$  incorporate more of all of the  $\alpha$ -olefin comonomers than the corresponding  $\text{C}_2$   $\text{Zr}_2^{\text{SiPr}_3}\text{-NMe}_2$  and  $\text{Zr}_1^{\text{SiPr}_3}\text{-NMe}_2$ , suggesting that the anthracene substituents are not as sterically bulky to the zirconium centers compared to methylated aryl substituents. Comparison of comonomer incorporation levels with

$\text{C}_2$  dinuclear vs mononuclear catalysts reveals a systematic trend. The dizirconium catalysts incorporate 1.4–2.1 times the small propylene comonomer compared to the mononuclear versions, but incorporate the larger 1-hexene comonomer similarly. With 1-tetradecene, however, both the dinuclear  $\text{C}_2$  catalysts incorporate less of the comonomer than the corresponding monozirconium catalysts (Figure 5). The  $\text{C}_s$

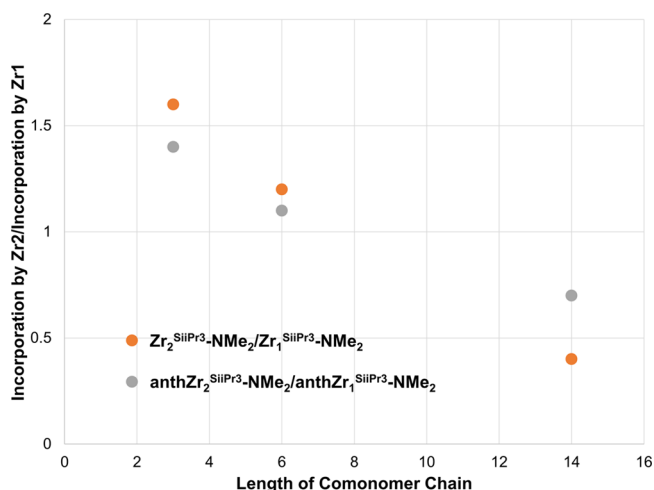


**Figure 5.** Plot of the ratio of comonomer incorporation by the bimetallic catalyst to monometallic catalyst according to the length of the comonomer.

$\text{Zr}_2^{\text{SiPr}_3}\text{-NMe}_2$  catalyst does not show a similar behavior. Overall, the  $\text{C}_2$  dinuclear catalysts relative to the mononuclear analogues show a decrease in comonomer incorporation with increasing size of the olefin (Figure 5). This is consistent with the distal steric bulk of the second metal disfavoring larger comonomer incorporation. This trend is inconsistent with the  $\alpha$ -olefin having an agostic interaction with the second metal center as previously proposed for dinuclear catalysts A (Figure 1).<sup>2</sup> The longer chain olefins are expected to be able to better accommodate such distal agostic interactions and incorporate in higher levels with dinuclear compared to mononuclear catalysts, which is not observed. The proposed steric effect is further supported by the difference in the magnitude of the effects between anthracene and tetramethylbenzene linkers. Plotting the ratio of  $\alpha$ -olefin incorporation with dinuclear vs mononuclear analogues, the tetramethylbenzene linker shows a more pronounced effect with the increasing size of the olefin, which correlates with a higher steric pressure on the incoming olefin from the methyl-substituted linker compared to flatter anthracene (Figure 5).

## SUMMARY

Mono- and dinuclear Zr benzyl complexes supported by pyridine bisphenolate and bisamine bisphenolate ligands featuring bulky  $\text{SiR}_3$  ( $\text{R} = ^i\text{Pr}, \text{Ph}$ ) substituents were prepared and studied for olefin polymerization catalysis. With these compounds, an extensive series of dinuclear olefin polymerization catalysts and their mononuclear analogues is available for structure function studies. Generally, the dinuclear systems show better control of tacticity, although only modest levels of isotacticity were achieved. The distal steric effect caused by the second metal is proposed to lead to improved tacticity control for dinuclear complexes. Of the ligands studied, the largest steric difference between the substituents on the two phenolate

ligands bound to the same metal correlates with best tacticity control. This results from a small rather than very large substituent on the phenoxide that is not connected to the linker. Ethylene- $\alpha$ -olefin copolymerization studies revealed that the longer chain olefins are incorporated at lower levels by dinuclear compared to mononuclear catalysts relative to shorter chain olefins. This effect is also consistent with steric effects caused by the second metal and not with a distal agostic interaction. Overall, the reported studies provide fundamental insight into the advantages of dinuclear vs mononuclear catalysts for olefin polymerization, in particular related to control of tacticity and comonomer incorporation.

## EXPERIMENTAL SECTION

**General Notes.** All air- and water-sensitive compounds were manipulated under  $N_2$  or Ar using standard Schlenk or glovebox techniques. Solvents for air- and moisture-sensitive reactions were dried by the method of Grubbs.<sup>16</sup> Chlorobenzene and 1-hexene for polymerization with stoichiometric activators were refluxed over  $CaH_2$  for greater than 72 h, vacuum transferred, and run over activated alumina plugs prior to use.  $[CPh_3][B(C_6F_5)_4]$  and  $[HNMe_2Ph][B(C_6F_5)_4]$  were purchased from Strem and used without further purification. Ethylene (99.999%) and propylene (99.999%) were passed through purification columns containing molecular sieves and oxygen scavenger. Toluene, 1-hexene, and 1-tetradecene for polymerizations were purchased from Sigma-Aldrich and dried over 4 Å molecular sieves prior to use. MAO (30 wt % in toluene) was purchased from Chemtura. Deuterated solvents were purchased from Cambridge Isotopes Lab, Inc.;  $CDCl_3$  and 1,1,2,2-tetrachloroethane- $d_2$  were used without further purification;  $C_6D_6$  was distilled from purple Na/benzophenone ketyl and filtered over activated alumina prior to use.  $^1H$  and  $^{13}C$  spectra were recorded on Varian Mercury 300, Varian INOVA-300, 400, or 500, or Bruker Cryoprobe 400 spectrometers.  $^1H$  and  $^{13}C$  chemical shifts are reported relative to residual solvent resonances. Elemental analysis was performed on a PerkinElmer 2400 CHNS/O analyzer, and samples were taken from representative batches prepared in an  $N_2$ -filled glovebox.

**Preparation of  $H_2^{SiPr^3-NMe_2}$ .** To a solution of **4** (613.4 mg, 1.508 mmol, 2.5 mmol) and  $NEt^tPr_2$  (0.21 mL, 1.506 mmol, 2.5 equiv) in THF (15 mL) at 0 °C was added **7** (375.8 mmol, 0.6096 mmol, 1 equiv) in THF (21 mL) over the course of several minutes. The reaction was stirred 3 h, with warming; then volatiles were removed under reduced pressure. The residue was dissolved in dichloromethane (DCM) and washed with  $K_2CO_3$  (2 $\times$ ), water, and brine. The combined organics were dried with  $MgSO_4$ , filtered, and evaporated. Purification by column chromatography (3:2 EtOAc–hexanes (v/v),  $R_f \sim 0.2$ ) and lyophilization from benzene afforded  $H_2^{SiPr^3-NMe_2}$  as a white solid (434.8 mg, 56.2%).  $^1H$  NMR (400 MHz,  $CDCl_3$ ):  $\delta$  9.53 (br s, 4H, OH), 7.34 (d,  $J = 2.9$  Hz, 2H, Ar-H), 7.15 (d,  $J = 2.2$  Hz, 2H, Ar-H), 7.08 (d,  $J = 2.2$  Hz, 2H, Ar-H), 7.05 (d,  $J = 2.4$  Hz, 2H, Ar-H), 3.78 (s, 4H,  $ArCH_2$ ), 3.74 (s, 4H,  $ArCH_2$ ), 2.66 (m, 4H,  $CH_2$ ), 2.57 (m, 4H,  $CH_2$ ), 2.24 (s, 12H,  $ArCH_3$ ), 2.00 (s, 12H,  $N(CH_3)_2$ ), 1.50 (m, 6H,  $SiCH(CH_3)_2$ ), 1.32 (s, 18H,  $C(CH_3)_3$ ), 1.31 (s, 18H,  $C(CH_3)_3$ ), 1.07 (d,  $J = 7.5$  Hz, 36H,  $SiCH(CH_3)_2$ ).  $^{13}C$  NMR (101 MHz,  $CDCl_3$ ):  $\delta$  160.47 (Ar), 151.31 (Ar), 141.62 (Ar), 140.25 (Ar), 137.48 (Ar), 133.73 (Ar), 133.06 (Ar), 129.40 (Ar), 128.16 (Ar), 127.63 (Ar), 126.48 (Ar), 121.90 (Ar), 120.63 (Ar), 120.41 (Ar), 58.16 ( $CH_2$ ), 56.95 ( $CH_2$ ), 55.57 ( $CH_2$ ), 49.81 ( $CH_2$ ), 45.32 ( $N(CH_3)_2$ ), 34.24 ( $ArC(CH_3)_3$ ), 34.08 ( $ArC(CH_3)_3$ ), 31.88 ( $ArC(CH_3)_3$ ), 19.27 ( $SiCH(CH_3)_2$ ), 17.99 ( $ArCH_3$ ), 11.94 ( $SiCH(CH_3)_2$ ). HRMS (FAB+): calcd for  $C_{80}H_{131}O_4N_4Si_2$  (M + H)<sup>+</sup> 1267.971, found 1267.970.

**Preparation of  $Zr_2^{SiPr^3-NMe_2}$  ( $C_s$  and  $C_2$  Symmetric).** Proligand  $H_2^{SiPr^3-NMe_2}$  (201.4 mg, 0.1588 mmol, 1 equiv) in toluene (2.5 mL) was added to a stirred solution of  $ZrBn_4$  (144.7 mg, 0.3175 mmol, 2 equiv) in toluene (3 mL), and the reaction stirred in the dark at room temperature for 3 h. Volatiles were removed *in vacuo*, and the crude material was fractionated between pentane, diethyl ether, and benzene.

The ether fraction afforded primarily the  $C_s$  symmetric isomer with ca. 12% of the  $C_2$  symmetric isomer (80.0 mg, 0.0442 mmol, 28%). The benzene fraction afforded primarily the  $C_2$  symmetric isomer, which was cleanly isolated following recrystallization from toluene–pentane (81.8 mg, 0.0452 mmol, 28%). X-ray quality crystals of the  $C_2$  isomer were grown by vapor diffusion of pentane into toluene at  $-35$  °C.  $Zr_2^{SiPr^3-NMe_2}$ :  $^1H$  NMR (400 MHz,  $C_6D_6$ ):  $\delta$  7.73 (d,  $J = 2.6$  Hz, 2H, Ar-H), 7.45 (d,  $J = 2.6$  Hz, 2H, Ar-H), 7.27 (m, 4H, Ar-H), 7.17 (d,  $J = 2.5$  Hz, 2H, Ar-H), 7.12 (d,  $J = 2.2$  Hz, 2H, Ar-H), 7.03 (m, 4H, Ar-H), 6.93 (m, 4H, Ar-H), 6.81 (t,  $J = 7.4$  Hz, 2H, Ar-H), 6.69 (t,  $J = 7.4$  Hz, 2H, Ar-H), 3.90 (d,  $J = 13.4$  Hz, 2H,  $CH_2$ ), 3.74 (d,  $J = 13.4$  Hz, 2H,  $CH_2$ ), 2.93 (s, 6H,  $ArCH_3$ ), 2.75 (d,  $J = 13.4$  Hz, 2H,  $ArCH_2$ ), 2.65 (d,  $J = 13.4$  Hz, 2H,  $ArCH_2$ ), 2.56 (s, 6H,  $ArCH_3$ ), 2.40 (m, 4H), 2.29 (m, 4H), 2.07–1.99 (m, 6H), 1.78 (m, 4H), 1.54–1.34 (m, 84H), 0.99 (br m, 2H).  $^{13}C$  NMR (101 MHz,  $CDCl_3$ ):  $\delta$  165.43 (Ar), 157.36 (Ar), 152.14 (Ar), 146.00 (Ar), 141.56 (Ar), 140.42 (Ar), 140.18 (Ar), 135.38 (Ar), 134.67 (Ar), 132.06 (Ar), 131.06 (Ar), 130.76 (Ar), 129.11 (Ar), 129.04 (Ar), 126.38 (Ar), 126.06 (Ar), 125.57 (Ar), 125.14 (Ar), 122.24 (Ar), 121.69 (Ar), 119.88 (Ar), 70.82 ( $CH_2$ ), 65.10 ( $CH_2$ ), 64.83 ( $CH_2$ ), 64.05 ( $CH_2$ ), 60.39 ( $CH_2$ ), 51.50 ( $CH_2$ ), 34.28 ( $C(CH_3)_3$ ), 34.16 ( $C(CH_3)_3$ ), 31.90 ( $C(CH_3)_3$ ), 20.30, 19.99, 19.89, 19.83, 19.39, 13.15 ( $SiCH(CH_3)_2$ ). Anal. Calcd for  $C_{108}H_{154}N_4O_4Si_2Zr_2$ : C, 71.63; H, 8.57, N, 3.09. Found: C, 71.65; H, 8.81; N, 3.41.  $C_2$   $Zr_2^{SiPr^3-NMe_2}$ :  $^1H$  NMR (500 MHz,  $CD_2Cl_2$ ):  $\delta$  7.42 (d,  $J = 2.2$  Hz, 2H, Ar-H), 7.18 (d,  $J = 2.3$  Hz, 2H, Ar-H), 7.08 (m, 4H, Ar-H), 7.02 (m, 6H, Ar-H), 6.99 (d,  $J = 2.2$  Hz, 2H, Ar-H), 6.83–6.77 (m, 6H, Ar-H), 6.63 (m, 6H, Ar-H), 3.62 (d,  $J = 13.5$  Hz, 2H,  $CH_2$ ), 3.42 (d,  $J = 13.5$  Hz, 2H,  $CH_2$ ), 2.85 (d,  $J = 13.9$  Hz, 2H,  $CH_2$ ), 2.77 (d,  $J = 13.7$  Hz, 2H,  $CH_2$ ), 2.66 (br m, 2H,  $CH_2$ ), 2.58 (s, 6H,  $ArCH_3$ ), 2.30 (br s, 2H,  $CH_2$ ), 2.25 (s, 6H,  $ArCH_3$ ), 2.04–1.99 (m, 4H,  $CH_2$ ), 1.89–1.84 (m, 6H), 1.78 (br m, 2H), 1.52 (m, 8H), 1.41 (m, 4H,  $CH_2$ ), 1.35 (m, 24H), 1.27 (m, 42H), 1.16 (d,  $J = 7.5$  Hz, 18H).  $^{13}C$  NMR (101 MHz,  $C_6D_6$ ):  $\delta$  165.46 (Ar), 157.04 (Ar), 152.93 (Ar), 144.27 (Ar), 141.30 (Ar), 140.60 (Ar), 139.50 (Ar), 135.33 (Ar), 134.84 (Ar), 132.23 (Ar), 131.40 (Ar), 130.15 (Ar), 129.46 (Ar), 129.33 (Ar), 126.15 (Ar), 125.79 (Ar), 125.70 (Ar), 124.75 (Ar), 122.71 (Ar), 121.58 (Ar), 119.86 (Ar), 67.61 ( $CH_2$ ), 64.79 ( $CH_2$ ), 64.07 ( $CH_2$ ), 63.87 ( $CH_2$ ), 60.00 ( $CH_2$ ), 51.37 ( $CH_2$ ), 34.32 ( $C(CH_3)_3$ ), 34.16 ( $C(CH_3)_3$ ), 31.93 ( $C(CH_3)_3$ ), 31.88 ( $C(CH_3)_3$ ), 22.75, 21.45, 20.33, 20.24, 19.83, 19.54, 14.31, 13.11 ( $SiCH(CH_3)_2$ ). Anal. Calcd for  $C_{108}H_{154}N_4O_4Si_2Zr_2$ : C, 71.63; H, 8.57, N, 3.09. Found: C, 72.01; H, 8.74; N, 3.12.

**Preparation of  $H_2^{ArSiPr^3-NMe_2}$ .** To a solution of **10** (1.21 g, 2.965 mmol, 1.25 equiv) and  $NEt^tPr_2$  (0.52 mL, 3.0 mmol, 1.25 equiv) in THF (45 mL) was added **7** (0.927 g, 2.38 mmol, 1 equiv) in THF (50 mL) over the course of several minutes. The reaction was stirred 3 h, with warming; then volatiles were removed under reduced pressure. The residue was dissolved in DCM and washed with  $K_2CO_3$  (2 $\times$ ), water, and brine, then dried with  $MgSO_4$ , filtered, and evaporated. Purification by column chromatography (5:1 EtOAc–hexanes (v/v)) and lyophilization from benzene afforded the prolignand as a white solid (1.1 g, 1.5 mmol, 65%).  $^1H$  NMR (400 MHz,  $CDCl_3$ ):  $\delta$  9.08 (br s, 2H, OH), 7.31 (d,  $J = 2.4$  Hz, 1H, Ar-H), 7.08 (d,  $J = 2.5$  Hz, 1H, Ar-H), 7.03 (d,  $J = 2.4$  Hz, 1H, Ar-H), 6.94 (d,  $J = 2.5$  Hz, 1H, Ar-H), 3.74 (s, 2H,  $CH_2$ ), 3.69 (s, 2H,  $CH_2$ ), 2.62 (m, 2H,  $CH_2$ ), 2.53 (m, 2H,  $CH_2$ ), 2.32 (s, 3H,  $ArCH_3$ ), 2.28 (s, 6H,  $ArCH_3$ ), 2.20 (s, 6H,  $ArCH_3$ ), 1.97 (s, 6H,  $N(CH_3)_2$ ), 1.48 (sept,  $J = 7.59$  Hz, 3H,  $CH(CH_3)_2$ ), 1.30 (s, 9H,  $C(CH_3)_3$ ), 1.28 (s, 9H,  $C(CH_3)_3$ ), 1.05 (d,  $J = 7.5$  Hz, 18H,  $CH(CH_3)_2$ ).  $^{13}C$  NMR (101 MHz,  $CDCl_3$ ):  $\delta$  160.27 (Ar), 151.71 (Ar), 141.40 (Ar), 140.32 (Ar), 136.72 (Ar), 133.88 (Ar), 133.82 (Ar), 132.84 (Ar), 132.16 (Ar), 129.81 (Ar), 127.73 (Ar), 126.34 (Ar), 121.65 (Ar), 120.69 (Ar), 120.29 (Ar), 58.16 ( $CH_2$ ), 56.95 ( $CH_2$ ), 55.99 ( $CH_2$ ), 49.66 ( $CH_2$ ), 45.36 ( $N(CH_3)_2$ ), 34.16 ( $C(CH_3)_3$ ), 34.07 ( $C(CH_3)_3$ ), 31.86 ( $C(CH_3)_3$ ), 19.27 ( $SiCH(CH_3)_2$ ), 18.27 ( $ArCH_3$ ), 17.13 ( $ArCH_3$ ), 16.85 ( $ArCH_3$ ), 11.96 ( $SiCH(CH_3)_2$ ). HRMS (FAB+): calcd for  $C_{46}H_{75}N_2O_2Si$  (M + H)<sup>+</sup> 715.5598, found 715.5579.

**Preparation of  $Zr_1^{ArSiPr^3-NMe_2}$ .** Proligand  $H_2^{ArSiPr^3-NMe_2}$  (137 mg, 0.191 mmol, 1.0 equiv) in toluene (3 mL) was added to a stirring solution of  $ZrBn_4$  (87.3 mg, 0.192 mmol, 1.0 equiv) in toluene (2 mL).

The reaction was stirred 3 h, in the dark; then volatiles removed *in vacuo* to afford a yellow solid. This was washed with 6 mL each of pentane and diethyl ether to afford the desired product (145 mg, 0.147 mmol, 76.7%). X-ray quality crystals were grown by slow evaporation of benzene at room temperature.  $^1\text{H}$  NMR (500 MHz,  $\text{C}_6\text{D}_6$ ):  $\delta$  7.72 (s, 1H, Ar-H), 7.31 (s, 1H, Ar-H), 7.24 (t,  $J = 7.2$  Hz, 2H, Ar-H), 7.07 (d,  $J = 6.6$  Hz, 2H, Ar-H), 7.01–6.6.95 (m, 5H, Ar-H), 6.85 (t,  $J = 7.2$  Hz, 2H, Ar-H), 6.64 (t,  $J = 7.2$  Hz, 1H, Ar-H), 3.82 (d,  $J = 13.5$  Hz, 1H,  $\text{CH}_2$ ), 3.59 (d,  $J = 13.5$  Hz, 1H,  $\text{CH}_2$ ), 2.66 (d,  $J = 13.5$  Hz, 1H,  $\text{CH}_2$ ), 2.62 (s, 3H, Ar $\text{CH}_3$ ), 2.61 (d, 1H,  $\text{CH}_2$ ), 2.45 (s, 3H, Ar $\text{CH}_3$ ), 2.43 (d, 1H,  $\text{CH}_2$ ), 2.39 (d,  $J = 10.1$  Hz, 1H,  $\text{CH}_2$ ), 2.30 (s, 6H, Ar $\text{CH}_3$ ), 2.26 (d,  $J = 9.8$  Hz, 1H,  $\text{CH}_2$ ), 2.19 (d,  $J = 9.8$  Hz, 1H,  $\text{CH}_2$ ), 2.14–2.07 (m, 7H), 1.90 (br m, 1H), 1.51–1.41 (m, 16H), 1.36–1.33 (m, 27H), 1.25 (br m, 1H).  $^{13}\text{C}$  NMR (126 MHz,  $\text{C}_6\text{D}_6$ ):  $\delta$  165.19 (Ar), 156.80 (Ar), 151.20 (Ar), 145.79 (Ar), 141.54 (Ar), 140.75 (Ar), 137.11 (Ar), 135.45 (Ar), 133.96 (Ar), 133.73 (Ar), 132.85 (Ar), 132.34 (Ar), 130.79 (Ar), 130.67 (Ar), 129.02 (Ar), 128.76 (Ar), 127.30 (Ar), 127.10 (Ar), 126.91 (Ar), 126.60 (Ar), 125.47 (Ar), 125.35 (Ar), 124.78 (Ar), 122.36 (Ar), 122.00 (Ar), 120.18 (Ar), 67.38 ( $\text{CH}_2$ ), 66.03 ( $\text{CH}_2$ ), 64.98 ( $\text{CH}_2$ ), 64.43 ( $\text{CH}_2$ ), 60.08 ( $\text{CH}_2$ ), 51.30 ( $\text{CH}_2$ ), 47.14 ( $\text{CH}_2$ ), 34.24 ( $\text{C}(\text{CH}_3)_3$ ), 34.19 ( $\text{C}(\text{CH}_3)_3$ ), 31.88 ( $\text{C}(\text{CH}_3)_3$ ), 20.33, 19.84, 19.40, 17.40, 16.98, 13.22 ( $\text{SiCH}(\text{CH}_3)_2$ ). Anal. Calcd for  $\text{C}_{60}\text{H}_{86}\text{N}_2\text{O}_2\text{SiZr}$ : C, 73.04; H, 8.79; N, 2.84. Found: C, 73.22; H, 8.96; N, 3.14.

**Preparation of anth $\text{H}_4$ <sup>SiPr $^3$</sup> -NMe $_2$ .** To a solution of 7 (1.539 g, 3.785 mmol, 2.5 equiv) were added  $\text{NEtPr}_2$  (0.658 mL, 3.78 mmol, 2.5 equiv) in THF (75 mL) at 0 °C and anth $\text{4}$  (1.008 g, 1.523 mmol, 1 equiv) in THF (40 mL) over the course of several minutes. The resulting red solution was stirred for 3 h, with warming; then volatiles were removed under reduced pressure. The residue was dissolved in DCM, washed with  $\text{K}_2\text{CO}_3$  (2 $\times$ ), water, and brine, dried with  $\text{MgSO}_4$ , filtered, and evaporated. Purification by column chromatography (3:2:1 EtOAc–hexanes–benzene (v/v/v)) afforded the desired proligand as a tan solid (1.16 g, 0.886 mmol, 58%).  $^1\text{H}$  NMR (400 MHz,  $\text{CDCl}_3$ ):  $\delta$  9.73 (br s, 4H, OH), 7.71–7.69 (m, 4H, anth-H), 7.36 (d,  $J = 2.8$  Hz, 2H, Ar-H), 7.35 (d,  $J = 2.8$  Hz, 2H, Ar-H), 7.32–7.30 (m, 4H, anth-H), 7.26 (d,  $J = 2.3$  Hz, 2H, Ar-H), 7.08 (d,  $J = 2.8$  Hz, 2H, Ar-H), 3.89 (s, 4H, Ar- $\text{CH}_2$ ), 3.83 (s, 4H, Ar- $\text{CH}_2$ ), 2.74 (m, 4H,  $\text{CH}_2$ ), 2.59 (m, 4H,  $\text{CH}_2$ ), 2.13 (s, 12H,  $\text{N}(\text{CH}_3)_2$ ), 1.42 (m, 6H,  $\text{SiCH}(\text{CH}_3)_2$ ), 1.35 (s, 18H,  $\text{C}(\text{CH}_3)_3$ ), 1.33 (s, 18H,  $\text{C}(\text{CH}_3)_3$ ), 1.00 (d,  $J = 7.5$  Hz, 36 H,  $\text{SiCH}(\text{CH}_3)_2$ ).  $^{13}\text{C}$  NMR (101 MHz,  $\text{CDCl}_3$ ):  $\delta$  160.51 (Ar), 152.66 (Ar), 141.79 (Ar), 140.25 (Ar), 134.17 (Ar), 133.87 (Ar), 130.61 (Ar), 129.80 (Ar), 127.85 (Ar), 127.32 (Ar), 127.27 (Ar), 125.82 (Ar), 124.96 (Ar), 122.41 (Ar), 121.03 (Ar), 120.31 (Ar), 57.72 ( $\text{CH}_2$ ), 56.82 ( $\text{CH}_2$ ), 55.47 ( $\text{CH}_2$ ), 49.60 ( $\text{CH}_2$ ), 45.27 ( $\text{N}(\text{CH}_3)_2$ ), 34.34 ( $\text{C}(\text{CH}_3)_3$ ), 34.09 ( $\text{C}(\text{CH}_3)_3$ ), 31.89 ( $\text{C}(\text{CH}_3)_3$ ), 19.16 ( $\text{SiCH}(\text{CH}_3)_2$ ), 11.90 ( $\text{SiCH}(\text{CH}_3)_2$ ). HRMS (FAB+): calcd for  $\text{C}_{84}\text{H}_{127}\text{N}_4\text{O}_4\text{Si}_4$ , 1311.94, found 1311.9396.

**Preparation of anth $\text{Zr}_2$ <sup>SiPr $^3$</sup> -NMe $_2$ .** A 20 mL scintillation vial was charged in the dark with a stirbar,  $\text{ZrBn}_4$  (113 mg, 0.248 mmol, 2 equiv), and 3 mL of toluene, and the solution was frozen in the glovebox cold well. A separate vial was charged with anth $\text{H}_4$ <sup>SiPr $^3$</sup> -NMe $_2$  (163 mg, 0.124 mmol, 1 equiv) dissolved in toluene (4 mL), and the solution frozen in the cold well. The thawing proligand solution was added to the top of the thawing  $\text{ZrBn}_4$  solution and then stirred, in the dark, with warming, for 3 h. Volatiles were removed, and the resulting yellow solid was recrystallized by pentane–benzene layering at room temperature to give the  $\text{C}_2$  symmetric complex as a yellow, crystalline solid (116 mg, 0.0626 mmol, 51%). X-ray quality crystals were grown by toluene–hexanes layering at –35 °C.  $^1\text{H}$  NMR (400 MHz,  $\text{C}_6\text{D}_6$ ):  $\delta$  8.84 (d,  $J = 8.5$  Hz, 2H, anthH), 8.12 (d,  $J = 9.1$  Hz, 2H, anthH), 7.70–7.63 (m, 4H, Ar-H), 7.59 (t,  $J = 7.1$  Hz, 2 H, Ar-H) 7.41 (t,  $J = 7.1$  Hz, 2H, Ar-H), 7.25 (d,  $J = 2.3$  Hz, 2H, Ar-H), 7.12 (d,  $J = 2.3$  Hz, 2H, Ar-H), 6.99 (m, 10H), 6.83 (br m, 4H), 6.70 (m, 4H), 6.43 (br m, 2H), 4.07 (d,  $J = 13.6$  Hz, 2H,  $\text{CH}_2$ ), 3.75 (d,  $J = 12.4$  Hz, 2H,  $\text{CH}_2$ ), 2.75 (d,  $J = 12.4$  Hz, 2H,  $\text{CH}_2$ ), 2.70 (d,  $J = 13.2$  Hz, 2H,  $\text{CH}_2$ ), 2.39 (br m, 2H), 2.04–1.91 (m, 10H), 1.80 (br m, 2H), 1.67 (d,  $J = 10.2$  Hz, 4H,  $\text{CH}_2$ ), 1.60 (br m, 2H) 1.46 (d,  $J = 7.52$  Hz, 18H), 1.36 (s, 18H), 1.31 (m, 42H) 1.19 (br s, 6H), 1.08 (br m, 2H).  $^{13}\text{C}\{^1\text{H}\}$  NMR (101 MHz,  $\text{C}_6\text{D}_6$ ):  $\delta$  165.50 (Ar), 157.91 (Ar), 153.07 (Ar), 143.63

(Ar), 141.53 (Ar), 140.60 (Ar), 136.22 (Ar), 135.40 (Ar), 133.09 (Ar), 131.69 (Ar), 131.12 (Ar), 130.29 (Ar), 129.88 (Ar), 129.34 (Ar), 128.60 (Ar), 127.23 (Ar), 126.67 (Ar), 126.33 (Ar), 126.25 (Ar), 125.71 (Ar), 125.58 (Ar), 124.71 (Ar), 122.41 (Ar), 121.59 (Ar), 119.85 (Ar), 68.12 ( $\text{CH}_2$ ), 64.86 ( $\text{CH}_2$ ), 63.92 ( $\text{CH}_2$ ), 63.73 ( $\text{CH}_2$ ), 60.15 ( $\text{CH}_2$ ), 51.37, 34.36 ( $\text{C}(\text{CH}_3)_3$ ), 34.19 ( $\text{C}(\text{CH}_3)_3$ ), 31.90 ( $\text{C}(\text{CH}_3)_3$ ), 31.83, 22.75, 20.25, 19.76, 14.31, 13.02. Anal. Calcd for  $\text{C}_{112}\text{H}_{150}\text{N}_4\text{O}_4\text{Si}_2\text{Zr}_2$ : C, 72.52; H, 8.15; N, 3.02. Found: C, 72.18; H, 8.35; N, 3.05.

**Preparation of anth $\text{H}_2$ <sup>ArSiPr $^3$</sup> -NMe $_2$ .** To a solution of anth $\text{10}$  (2.384 g, 5.861 mmol, 1.25 equiv) and  $\text{NEtPr}_2$  (1.02 mL, 5.86 mmol, 1.25 equiv) in THF (150 mL) at 0 °C was added 7 (2.035 g, 4.695 mmol, 1 equiv) in THF (100 mL) over the course of several minutes. The resulting red solution was stirred 3 h, with warming; then volatiles were removed under reduced pressure. The residue was taken up in DCM and washed with  $\text{K}_2\text{CO}_3$  (2 $\times$ ), water, and brine, then dried with  $\text{MgSO}_4$ , filtered, and evaporated. Purification by column chromatography (3:1 EtOAc–hexanes (v/v)) and lyophilization from benzene afforded the desired proligand as a tan solid (1.233 g, 1.624 mmol, 35%).  $^1\text{H}$  NMR (500 MHz,  $\text{CDCl}_3$ ):  $\delta$  9.81 (br s, 2H, OH), 8.36 (d,  $J = 8.7$  Hz, 2H, anth-H), 7.66 (d,  $J = 8.7$  Hz, 2H, anth-H), 7.50 (dd, 2H, anth-H), 7.31 (m, 4H, anth-H and Ar-H), 7.20 (d,  $J = 2.4$  Hz, 1H, Ar-H), 7.06 (d,  $J = 2.5$  Hz, 1H, Ar-H), 3.84 (s, 2H, Ar $\text{CH}_2$ ), 3.76 (s, 2H, Ar $\text{CH}_2$ ), 3.19 (s, 3H, anth $\text{CH}_3$ ), 2.70 (m, 2H,  $\text{CH}_2$ ), 2.55 (m, 2H,  $\text{CH}_2$ ), 2.07 (s, 6H,  $\text{N}(\text{CH}_3)_2$ ), 1.37 (m, 3H,  $\text{SiCH}(\text{CH}_3)_2$ ), 1.33 (s, 9H,  $\text{C}(\text{CH}_3)_3$ ), 1.31 (s, 9H,  $\text{C}(\text{CH}_3)_3$ ), 0.93 (d, 18H,  $J = 7.5$  Hz,  $\text{SiCH}(\text{CH}_3)_2$ ).  $^{13}\text{C}$  NMR (126 MHz,  $\text{CDCl}_3$ ):  $\delta$  160.29 (Ar), 153.04 (Ar), 141.54 (Ar), 140.20 (Ar), 134.00 (Ar), 133.37 (Ar), 130.49 (Ar), 130.09 (Ar), 129.84 (Ar), 129.76 (Ar), 128.54 (Ar), 128.13 (Ar), 128.03 (Ar), 126.99 (Ar), 126.01 (Ar), 124.96 (Ar), 124.77 (Ar), 124.57 (Ar), 122.22 (Ar), 121.31 (Ar), 120.19 (Ar), 57.28 ( $\text{CH}_2$ ), 56.74 ( $\text{CH}_2$ ), 56.26 ( $\text{CH}_2$ ), 49.44 ( $\text{CH}_2$ ), 45.16 ( $\text{N}(\text{CH}_3)_2$ ), 34.28 ( $\text{C}(\text{CH}_3)_3$ ), 34.06 ( $\text{C}(\text{CH}_3)_3$ ), 31.89 ( $\text{C}(\text{CH}_3)_3$ ), 19.09 ( $\text{SiCH}(\text{CH}_3)_2$ ), 14.41 (anth $\text{CH}_2$ ), 11.85 ( $\text{SiCH}(\text{CH}_3)_2$ ). HRMS (FAB+): calcd for  $\text{C}_{50}\text{H}_{71}\text{SiN}_2\text{O}_2$  (M + H) $^+$  759.5285, found 759.5264.

**Preparation of anth $\text{Zr}_1$ <sup>ArSiPr $^3$</sup> -NMe $_2$ .** Proligand anth $\text{H}_2$ <sup>ArSiPr $^3$</sup> -NMe $_2$  (200.0 mg, 0.2634 mmol, 1 equiv) in 4 mL of toluene was added to the top of a stirred solution of  $\text{ZrBn}_4$  (119.9 mg, 0.2631 mmol, 1 equiv) in 3 mL of toluene and stirred for 3 h in the dark. Volatiles were removed *in vacuo*, and the resulting yellow solid was washed with pentane and ether to afford the desired complex (140 mg, 0.136 mmol, 52%).  $^1\text{H}$  NMR (500 MHz,  $\text{C}_6\text{D}_6$ ):  $\delta$  8.44 (d,  $J = 9.1$  Hz, 1H, anth-H), 8.41 (d,  $J = 9.1$  Hz, 1H, anth-H), 8.33 (d,  $J = 9.1$  Hz, 1H, anth-H), 8.00 (d,  $J = 9.0$  Hz, 1H, anth-H), 7.69 (d,  $J = 2.4$  Hz, 1H, Ar-H), 7.57 (d,  $J = 2.2$  Hz, 1H, Ar-H), 7.51 (m, 2H, anth-H), 7.38 (m, 1H, anth-H), 7.22 (m, 2H, Ar-H), 7.12 (d,  $J = 2.2$  Hz, 1H, Ar-H), 6.97–6.93 (m, 4H, Ar-H), 6.89–6.83 (m, 3H, Ar-H), 6.70 (m, 1H, anth-H), 6.13 (d,  $J = 6.9$  Hz, 2H, Ar-H), 4.01 (d,  $J = 13.3$  Hz, 1H,  $\text{CH}_2$ ), 3.46 (d,  $J = 13.3$  Hz, 1H,  $\text{CH}_2$ ), 2.99 (s, 3H, anth $\text{CH}_3$ ), 2.70 (2d,  $J = 13.3$  Hz, 2H,  $\text{CH}_2$ ), 2.30 (br m, 1H,  $\text{CH}_2$ ), 2.11 (d,  $J = 10.2$  Hz, 1H,  $\text{CH}_2$ ), 2.00–1.89 (m, 5H), 1.53 (m, 1H,  $\text{CH}_2$ ), 1.49 (d,  $J = 9.3$  Hz, 1H,  $\text{CH}_2$ ), 1.46 (d,  $J = 9.3$  Hz, 1H,  $\text{CH}_2$ ), 1.41–1.36 (m, 18 H), 1.32–1.26 (m, 25H).  $^{13}\text{C}$  NMR (126 MHz,  $\text{C}_6\text{D}_6$ ):  $\delta$  165.30 (Ar), 157.86 (Ar), 151.74 (Ar), 143.57 (Ar), 141.82 (Ar), 140.66 (Ar), 135.41 (Ar), 134.20 (Ar), 131.49 (Ar), 131.41 (Ar), 130.95 (Ar), 130.75 (Ar), 130.58 (Ar), 129.01 (Ar), 126.96 (Ar), 126.77 (Ar), 126.50 (Ar), 126.21 (Ar), 125.98 (Ar), 125.91 (Ar), 125.79 (Ar), 125.37 (Ar), 124.77 (Ar), 124.68 (Ar), 124.08 (Ar), 122.64 (Ar), 121.86 (Ar), 120.00 (Ar), 66.14 ( $\text{CH}_2$ ), 65.07 ( $\text{CH}_2$ ), 64.61 ( $\text{CH}_2$ ), 64.19 ( $\text{CH}_2$ ), 60.09 ( $\text{CH}_2$ ), 51.64, 47.47, 34.33, 34.18, 31.86, 20.19, 19.70, 14.31, 13.06. Anal. Calcd for  $\text{C}_{64}\text{H}_{82}\text{N}_2\text{O}_2\text{SiZr}$ : C, 74.58; H, 8.02; N, 2.72. Found: C, 74.25; H, 8.17; N, 2.64.

**Preparation of 11.** Bis-syn-13-MOM (6.12 g, 11.8 mmol),  $\text{N,N,N',N'}$ -tetramethylethylenediamine (1.77 mL, 11.8 mmol), and THF (80 mL) were added to a Schlenk tube under inert atmosphere and cooled to –78 °C using a dry ice–acetone cooling bath. *n*-Butyllithium (2.5 M solution in hexane, 10.4 mL, 26.0 mmol) was added dropwise to the reaction solution and stirred while it warmed to room temperature for 4 h. The resulting orange-red solution was recooled to –78 °C, and trimethyl borate (3.95 mL, 35.4 mmol) was

added dropwise to the reaction mixture. After 30 min of stirring at  $-78^{\circ}\text{C}$ , the reaction mixture was allowed to warm to room temperature and stirred for 15 h. A saturated aqueous solution of  $\text{NH}_4\text{Cl}$  (30 mL) was added to quench the reaction. The crude product was extracted with diethyl ether (3 times), washed with brine (2 times), dried over anhydrous  $\text{MgSO}_4$ , and filtered, and volatiles were evaporated to dryness. The residue was dissolved in THF (80 mL), and NaI (5.31 g, 35.4 mmol) and trimethylsilyl chloride (4.49 mL, 35.4 mmol) were added to the solution. The resulting mixture was stirred at room temperature for 15 h. The product was extracted with diethyl ether (3 times), washed with water and brine, dried over  $\text{MgSO}_4$ , filtered, and concentrated *in vacuo*. The crude product was precipitated from MeOH and dried under vacuum. This crude slightly yellow powder (3.2 g, 6.2 mmol, 52% yield) was used for the subsequent Suzuki coupling reaction without further purification.

**Preparation of 12.** A mixture of boronic acid 14 (2 g, 3.9 mmol), 2-bromo-6-chloropyridine (1.47 g, 7.72 mmol), and potassium carbonate (3.20 g, 23.2 mmol) was dissolved in a mixture of toluene (40 mL), ethanol (13 mL), and water (13 mL). The reaction mixture was degassed via three freeze–pump–thaw cycles; then tetrakis(triphenylphosphine)palladium(0) (0.223 g, 0.193 mmol) was added, and the resulting yellow solution was stirred at  $75^{\circ}\text{C}$  for 24 h. The organic layer was separated, and the aqueous layer was extracted with ethyl acetate. The combined organic layers were washed with brine, dried over anhydrous  $\text{MgSO}_4$ , filtered, and concentrated to dryness. Purification by flash column chromatography on silica gel using  $\text{CH}_2\text{Cl}_2$ –hexanes as the eluent ( $v/v = 1:1$ ) gave a slightly yellow solid in 85% yield (2.15 g, 3.29 mmol).  $^1\text{H}$  NMR (400 MHz,  $\text{CDCl}_3$ ,  $25^{\circ}\text{C}$ ):  $\delta$  12.43 (s, 2H, OH), 7.91 (d,  $J = 8.0$  Hz, 2H, CH of py), 7.80 (t,  $J = 7.9$  Hz, 2H, CH of py), 7.78 (d,  $J = 2.5$  Hz, 2H, CH of a phenol ring), 7.31 (d,  $J = 2.4$  Hz, 2H, CH of a phenol ring), 7.24 (d,  $J = 7.7$  Hz, 2H, CH of py), 2.08 (s, 12H,  $\text{CH}_3$  of Ar), 1.39 (s, 18H,  $\text{CH}_3$  of  $^t\text{Bu}$ ).  $^{13}\text{C}$  NMR (101 MHz,  $\text{CDCl}_3$ ,  $25^{\circ}\text{C}$ ):  $\delta$  159.3 (py), 154.4 (phenol ring), 148.5 (py), 141.4 (phenol ring), 139.9 (CH of py), 137.6 (Ar), 132.5 (Ar), 131.8 (phenol ring), 131.7 (CH of phenol ring), 121.8 (CH of a phenol ring), 121.5 (CH of py), 118.0 (phenol ring), 117.5 (CH of py), 34.4 ( $\text{C}(\text{CH}_3)_3$  of  $^t\text{Bu}$ ), 31.7 ( $\text{CH}_3$  of  $^t\text{Bu}$ ), 18.0 ( $\text{CH}_3$  of Ar). HRMS (EI+): calcd for  $\text{C}_{40}\text{H}_{43}\text{Cl}_2\text{N}_2\text{O}_2$  ( $M + \text{H}$ ) $^+$  653.2702, found 653.2715.

**Preparation of  $\text{pyH}_4^{\text{SiPr}_3}$ .** A mixture of 15 (1.3 g, 2.0 mmol), boronic acid 11 (2.25 g, 4.98 mmol), and potassium carbonate (1.65 g, 11.9 mmol) was dissolved in a mixture of toluene (40 mL), ethanol (13 mL), and water (13 mL). The reaction mixture was degassed via three freeze–pump–thaw cycles, and then, tetrakis(triphenylphosphine)palladium(0) (0.12 g, 0.10 mmol) was added. The resulting yellow solution was stirred at  $75^{\circ}\text{C}$  for 24 h. The organic layer was separated, and the aqueous layer was extracted with ethyl acetate. The combined organic layers were washed with brine, dried over anhydrous  $\text{MgSO}_4$ , filtered, and concentrated to dryness. Purification by flash column chromatography on silica gel using  $\text{CH}_2\text{Cl}_2$ –hexanes as the eluent ( $v/v = 1:1$ ) gave a slightly yellow solid in 27% yield.  $^1\text{H}$  NMR (400 MHz,  $\text{CDCl}_3$ ,  $25^{\circ}\text{C}$ ):  $\delta$  12.84 (s, 2H, OH), 7.95–7.92 (m, 4H, py and a phenol ring), 7.88 (d,  $J = 2.5$  Hz, 2H, a phenol ring), 7.81–7.76 (m, 2H, py), 7.73 (d,  $J = 2.4$  Hz, 2H, a phenol ring), 7.52 (d,  $J = 2.4$  Hz, 2H, a phenol ring), 7.36 (s, 2H, OH), 7.22 (d,  $J = 2.4$  Hz, 2H, py), 2.11 (s, 12H,  $\text{CH}_3$  of Ar), 1.56 (sept,  $J = 7.5$  Hz, 6H, CH of  $^i\text{Pr}$ ), 1.39 (s, 18H,  $\text{CH}_3$  of  $^t\text{Bu}$ ), 1.37 (s, 18H,  $\text{CH}_3$  of  $^t\text{Bu}$ ), 1.13 (d,  $J = 7.5$  Hz, 36H,  $\text{CH}_3$  of  $^i\text{Pr}$ ).  $^{13}\text{C}$  NMR (101 MHz,  $\text{CDCl}_3$ ,  $25^{\circ}\text{C}$ ):  $\delta$  161.4, 158.1, 154.6, 149.7, 143.4, 140.5, 138.7 (CH), 136.8 (CH), 136.4, 134.1, 129.4 (py), 125.5 (CH), 124.7 (CH), 123.2, 122.9, 121.3 (CH), 118.6, 118.4 (CH), 34.6 ( $\text{C}(\text{CH}_3)_3$  or  $^t\text{Bu}$ ), 34.3 ( $\text{C}(\text{CH}_3)_3$  or  $^t\text{Bu}$ ), 31.7 ( $\text{CH}_3$  of  $^t\text{Bu}$ ), 31.7 ( $\text{CH}_3$  of  $^t\text{Bu}$ ), 19.2 ( $\text{CH}_3$  of  $^i\text{Pr}$ ), 18.0 ( $\text{CH}_3$  of Ar), 12.0 (CH of  $^i\text{Pr}$ ). HRMS (EI+): calcd for  $\text{C}_{78}\text{H}_{109}\text{N}_2\text{O}_4\text{Si}_2$  ( $M + \text{H}$ ) $^+$  1193.7926, found 1193.7931.

**Preparation of  $\text{pyZr}_1^{\text{SiPr}_3}$ .**  $\text{pyH}_4^{\text{SiPr}_3}$  (100 mg, 83.8  $\mu\text{mol}$ ) and  $\text{ZrBn}_4$  (76.1 mg, 168  $\mu\text{mol}$ ) were used for the reaction in benzene (quantitative yield).  $^1\text{H}$  NMR (300 MHz,  $\text{C}_6\text{D}_6$ ):  $\delta$  7.84 (d,  $J = 2.6$  Hz, 2H, ArH of phenol), 7.47 (d,  $J = 2.3$  Hz, 2H, ArH of phenol), 7.37 (d,  $J = 2.6$  Hz, 2H, ArH of phenol), 7.30 (d,  $J = 7.3$  Hz, 2H, pyH), 7.23 (d,  $J = 2.4$  Hz, 2H, ArH of phenol), 7.13 (d,  $J = 7.5$  Hz, 2H, pyH), 6.96 (t,

$J = 7.7$  Hz, 2H, pyH), 6.87–6.81 (m, 16H, BnH), 6.66 (m, 4H, BnH), 2.56 (s, 12H, Ar $\text{CH}_3$ ), 2.39 (d,  $J = 9.2$  Hz, 4H,  $\text{CH}_2\text{Ph}$ ), 2.27 (d,  $J = 9.2$  Hz, 4H,  $\text{CH}_2\text{Ph}$ ), 2.04 (sept,  $J = 7.6$  Hz, 6H, SiCH( $\text{CH}_3$ ) $_2$ ), 1.42 (d,  $J = 7.6$  Hz, 36H, SiCH( $\text{CH}_3$ ) $_2$ ), 1.40 (s, 18H,  $\text{C}(\text{CH}_3)_3$ ), 1.33 (s, 18H,  $\text{C}(\text{CH}_3)_3$ ).  $^{13}\text{C}$  NMR (101 MHz,  $\text{C}_6\text{D}_6$ ,  $25^{\circ}\text{C}$ ):  $\delta$  161.0, 160.6, 159.6, 153.6, 142.0, 141.0, 140.7, 139.8, 137.9, 137.1, 133.6, 132.7, 131.1, 130.2, 129.6, 128.8, 128.6, 126.8, 126.2, 124.4, 123.5, 122.9, 122.6, 62.4 ( $\text{CH}_2$  of Bn), 34.5 ( $\text{C}(\text{CH}_3)_3$  of  $^t\text{Bu}$ ), 34.3 ( $\text{C}(\text{CH}_3)_3$  of  $^t\text{Bu}$ ), 31.8 ( $\text{CH}_3$  of  $^t\text{Bu}$ ), 31.8 ( $\text{CH}_3$  of  $^t\text{Bu}$ ), 19.9 ( $\text{CH}_3$  of  $^i\text{Pr}$ ), 19.4 ( $\text{CH}_3$  of Ar), 13.2 (CH of  $^i\text{Pr}$ ). Anal. Calcd for  $\text{C}_{106}\text{H}_{132}\text{N}_2\text{O}_4\text{Si}_2\text{Zr}_2$ : C, 73.30; H, 7.66; N, 1.61. Found: C, 72.21; H, 7.51; N, 1.76.

**Preparation of  $\text{pyH}_2^{\text{ArSiPr}_3}$ .** Synthesis of  $\text{pyH}_2^{\text{ArSiPr}_3}$  was identical to that of  $\text{pyH}_4^{\text{SiPh}_3}$  except that boronic acid 15 $^{\text{iPr}}$  was used as a coupling partner for the Suzuki coupling reaction (55% yield).  $^1\text{H}$  NMR (400 MHz,  $\text{CDCl}_3$ ,  $25^{\circ}\text{C}$ ):  $\delta$  13.10 (s, 1H, OH), 7.95–7.88 (m, 2H), 7.84 (d,  $J = 2.5$  Hz, 1H), 7.79 (dd,  $J = 7.3$ , 1.8 Hz, 1H), 7.75 (d,  $J = 2.4$  Hz, 1H), 7.53 (d,  $J = 2.4$  Hz, 1H), 7.16 (d,  $J = 2.5$  Hz, 1H), 6.89 (s, 1H, OH), 2.33 (s, 3H,  $\text{CH}_3$  of Ar), 2.30 (s, 6H,  $\text{CH}_3$  of Ar), 2.07 (s, 6H,  $\text{CH}_3$  of Ar), 1.58 (sept,  $J = 14.8$ , 7.4 Hz, 3H, CH of  $^i\text{Pr}$ ), 1.38 (s, 9H,  $\text{CH}_3$  of  $^t\text{Bu}$ ), 1.37 (s, 9H,  $\text{CH}_3$  of  $^t\text{Bu}$ ), 1.15 (d,  $J = 7.5$  Hz, 18H,  $\text{CH}_3$  of  $^i\text{Pr}$ ).  $^{13}\text{C}$  NMR (101 MHz,  $\text{CDCl}_3$ ,  $25^{\circ}\text{C}$ ):  $\delta$  161.7, 158.1, 154.5, 149.5, 143.3, 140.4, 138.5 (CH), 136.8 (CH), 135.3, 133.6, 133.2, 133.2, 129.9, 129.5 (CH), 125.4 (CH), 124.5 (CH), 123.2, 123.0, 121.3 (CH), 118.3, 118.2 (CH), 34.5, 34.3, 31.7, ( $\text{CH}_3$  of  $^t\text{Bu}$ ), 31.6, ( $\text{CH}_3$  of  $^t\text{Bu}$ ), 19.2 ( $\text{CH}_3$  of  $^i\text{Pr}$ ), 18.2 ( $\text{CH}_3$  of Ar), 17.0 ( $\text{CH}_3$  of Ar), 16.9 ( $\text{CH}_3$  of Ar), 12.0. HRMS (EI+): calcd for  $\text{C}_{45}\text{H}_{64}\text{NO}_2\text{Si}$  ( $M + \text{H}$ ) $^+$  678.4706, found 678.4712.

**Preparation of  $\text{pyZr}_1^{\text{ArSiPr}_3}$ .**  $\text{pyH}_2^{\text{ArSiPr}_3}$  (676 mg, 0.998 mmol) and  $\text{ZrBn}_4$  (453 mg, 0.998 mmol) were used for the reaction in benzene (quantitative yield).  $^1\text{H}$  NMR (400 MHz,  $\text{C}_6\text{D}_6$ ,  $25^{\circ}\text{C}$ ):  $\delta$  7.87 (d,  $J = 2.5$  Hz, 1H), 7.40 (d,  $J = 2.4$  Hz, 1H), 7.29 (dd,  $J = 2.5$ , 1.6 Hz, 2H, CH of Bn), 7.26 (dd,  $J = 7.8$ , 1.1 Hz, 1H, CH of py), 7.23 (dd,  $J = 7.9$ , 1.0 Hz, 1H, CH of py), 6.95 (t,  $J = 7.9$  Hz, 1H, CH of py), 6.82 (t,  $J = 7.4$  Hz, 4H, CH of Bn), 6.73 (t,  $J = 7.2$  Hz, 2H), 6.53 (d,  $J = 7.3$  Hz, 4H, CH of Bn), 2.29 (br s, 15H,  $\text{CH}_3$  of Ar), 2.19 (d,  $J = 8.9$  Hz, 2H,  $\text{CH}_2$  of Bn), 2.02 (sept,  $J = 7.5$  Hz, 3H, CH of  $^i\text{Pr}$ ), 1.91 (d,  $J = 9.0$  Hz, 2H,  $\text{CH}_2$  of Bn), 1.39 (s, 9H,  $\text{CH}_3$  of  $^t\text{Bu}$ ), 1.39 (d,  $J = 7.7$  Hz, 18H,  $\text{CH}_3$  of  $^i\text{Pr}$ ), 1.33 (s, 9H,  $\text{CH}_3$  of  $^t\text{Bu}$ ).  $^{13}\text{C}$  NMR (101 MHz,  $\text{C}_6\text{D}_6$ ,  $25^{\circ}\text{C}$ ):  $\delta$  161.2, 161.1, 159.9, 153.0, 142.3, 141.4, 140.3, 140.2 (CH of py), 137.5, 137.0 (CH), 134.2, 132.7, 132.6, 131.5, 131.2 (CH), 130.6, 129.9 (CH of Bn), 129.5 (CH of Bn), 128.6, 127.1, 126.9 (CH of Bn), 126.7, 124.4 (CH of py), 123.7 (CH of py), 123.2, 123.0 (CH), 59.2 ( $\text{CH}_2$  of Bn), 34.4 ( $\text{C}(\text{CH}_3)_3$  of  $^t\text{Bu}$ ), 34.3 ( $\text{C}(\text{CH}_3)_3$  of  $^t\text{Bu}$ ), 31.8 (two set of  $\text{CH}_3$  of  $^t\text{Bu}$ ), 19.8 ( $\text{CH}_3$  of  $^i\text{Pr}$ ), 18.9 ( $\text{CH}_3$  of Ar), 17.0 ( $\text{CH}_3$  of Ar), 16.9 ( $\text{CH}_3$  of Ar), 13.4 (CH of  $^i\text{Pr}$ ). Anal. Calcd for  $\text{C}_{59}\text{H}_{75}\text{NO}_2\text{SiZr}$ : C, 74.63; H, 7.96; N, 1.48. Found: C, 75.15; H, 8.00; N, 1.65.

**Preparation of  $\text{pyH}_4^{\text{SiPh}_3}$ .** A mixture of 12 (1.3 g, 2.0 mmol), 11 $^{\text{SiPh}_3}$  (2.25 g, 4.98 mmol), and potassium carbonate (1.65 g, 11.9 mmol) was dissolved in a mixture of toluene (40 mL), ethanol (13 mL), and water (13 mL). The reaction mixture was degassed via three freeze–pump–thaw cycles. Then tetrakis(triphenylphosphine)palladium(0) (0.12 g, 99.7  $\mu\text{mol}$ ) was added, and the resulting yellow solution was stirred at  $75^{\circ}\text{C}$  for 24 h. The organic layer was separated, and the aqueous layer was extracted with ethyl acetate. The combined organic layers were washed with brine, dried over anhydrous  $\text{MgSO}_4$ , filtered, and concentrated to dryness. Purification by flash column chromatography on silica gel using  $\text{CH}_2\text{Cl}_2$ –hexanes as the eluent ( $v/v = 1:1$ ) gave a slightly yellow solid in 45% yield (1.25 g, 0.895 mmol).  $^1\text{H}$  NMR (400 MHz,  $\text{CDCl}_3$ ,  $25^{\circ}\text{C}$ ):  $\delta$  12.26 (s, 2H, OH), 7.87–7.79 (m, 4H), 7.73 (d,  $J = 2.5$  Hz, 2H), 7.69 (dd,  $J = 7.7$ , 1.4 Hz, 2H), 7.65 (d,  $J = 2.5$  Hz, 2H), 7.61–7.56 (m, 14H), 7.29–7.26 (m, 4H), 7.25–7.20 (m, 14H), 7.16 (s, 2H, OH), 7.09 (d,  $J = 2.5$  Hz, 2H, py), 1.94 (s, 12H,  $\text{CH}_3$  of Ar), 1.21 (s, 18H,  $\text{CH}_3$  of  $^t\text{Bu}$ ), 1.12 (s, 18H,  $\text{CH}_3$  of  $^t\text{Bu}$ ).  $^{13}\text{C}$  NMR (101 MHz,  $\text{CDCl}_3$ ,  $25^{\circ}\text{C}$ ):  $\delta$  160.9, 157.5, 155.2, 149.9, 143.2, 141.4, 138.6 (CH), 138.0 (CH), 136.6 (CH), 136.5 (CH), 135.2 (CH), 134.0, 129.6 (CH), 129.5, 129.3 (CH), 127.7 (CH), 126.6 (CH), 125.2 (CH), 122.6, 122.0, 121.5 (CH), 119.7, 118.7 (CH), 34.5 ( $\text{C}(\text{CH}_3)_3$  of  $^t\text{Bu}$ ), 34.3 ( $\text{C}(\text{CH}_3)_3$  of  $^t\text{Bu}$ ), 31.7

(CH<sub>3</sub> of <sup>t</sup>Bu), 31.6 (CH<sub>3</sub> of <sup>t</sup>Bu), 18.1 (CH<sub>3</sub> of Ar). HRMS (EI<sup>+</sup>): calcd for C<sub>96</sub>H<sub>97</sub>N<sub>2</sub>O<sub>4</sub>Si<sub>2</sub> (M + H)<sup>+</sup> 1397.6987, found 1397.7026.

**Preparation of pyZr<sub>2</sub><sup>ArSiPh<sub>3</sub></sup>.** pyH<sub>4</sub><sup>SiPh<sub>3</sub></sup> (100 mg, 71.6 μmol) in benzene (3 mL) was slowly added to a solution of ZrBn<sub>4</sub> (65.0 mg, 143 μmol) in benzene (2 mL) under dark conditions. The resulting solution was stirred for 5 h at room temperature. All volatiles were removed under vacuum to give a yellow powder (quantitative yield). <sup>1</sup>H NMR (300 MHz, C<sub>6</sub>D<sub>6</sub>): δ 8.01–7.97 (m, 12H, SiPh<sub>3</sub>), 7.71 (d, *J* = 2.4 Hz, 2H, ArH of phenol), 7.46 (d, *J* = 2.6 Hz, 2H, ArH of phenol), 7.39 (d, *J* = 2.5 Hz, 2H, ArH of phenol), 7.32 (d, *J* = 2.5 Hz, 2H, ArH of phenol), 7.29–7.21 (m, 22H, SiPh<sub>3</sub> and pyH), 6.99 (t, *J* = 8.3 Hz, 2H, pyH), 6.73–6.63 (m, 12H, BnH), 6.37 (m, 8H, BnH), 2.48 (s, 12H, ArCH<sub>3</sub>), 1.78 (d, *J* = 8.9 Hz, 4H, CH<sub>2</sub>Ph), 1.29 (s, 18H, C(CH<sub>3</sub>)<sub>3</sub>), 1.25 (s, 18H, C(CH<sub>3</sub>)<sub>3</sub>), 1.15 (d, *J* = 8.9 Hz, 4H, ArCH<sub>2</sub>). <sup>13</sup>C NMR (101 MHz, C<sub>6</sub>D<sub>6</sub>, 25 °C): δ 161.4, 160.2, 160.0, 153.5, 142.0, 141.9, 141.7, 140.3, 139.6, 139.5, 137.2, 137.1, 135.7, 133.6, 133.2, 131.8, 130.5, 130.1, 129.8, 128.8, 128.6, 127.0, 126.2, 124.2, 124.0, 122.4, 121.8, 60.5 (CH<sub>2</sub> of Bn), 38.2 (two sets of C(CH<sub>3</sub>)<sub>3</sub> of <sup>t</sup>Bu), 31.7 (CH<sub>3</sub> of <sup>t</sup>Bu), 31.6 (CH<sub>3</sub> of <sup>t</sup>Bu), 19.4 (CH<sub>3</sub> of Ar). Anal. Calcd for C<sub>124</sub>H<sub>120</sub>N<sub>2</sub>O<sub>4</sub>Si<sub>2</sub>Zr<sub>2</sub>: C, 76.73; H, 6.23; N, 1.44. Found: C, 76.67; H, 6.62; N, 1.39.

**Preparation of pyH<sub>2</sub><sup>ArSiPh<sub>3</sub></sup>.** A mixture of **18** (2.63 g, 6.46 mmol), **11** (2.92 g, 6.45 mmol), and potassium carbonate (2.68 g, 19.4 mmol) was dissolved in a mixture of toluene (40 mL), ethanol (13 mL), and water (13 mL). The reaction mixture was degassed via three freeze–pump–thaw cycles. Then tetrakis(triphenylphosphine)palladium(0) (0.370 g, 0.320 mmol) was added, and the resulting yellow solution was stirred at 75 °C for 24 h. The organic layer was separated, and the aqueous layer was extracted with ethyl acetate. The combined organic layers were washed with brine, dried over anhydrous MgSO<sub>4</sub>, filtered, and concentrated to dryness. Purification by flash column chromatography on silica gel using CH<sub>2</sub>Cl<sub>2</sub>–hexanes as the eluent (*v/v* = 1:5) gave a slightly yellow solid in 48% yield (2.42 g, 3.10 mmol). <sup>1</sup>H NMR (400 MHz, CDCl<sub>3</sub>, 25 °C): δ 7.92 (t, *J* = 7.9 Hz, 1H), 7.85 (dd, *J* = 7.9, 0.8 Hz, 1H), 7.82 (d, *J* = 2.5 Hz, 1H), 7.77 (d, *J* = 7.3 Hz, 1H), 7.70–7.67 (m, 7H), 7.39–7.35 (m, 3H), 7.33 (dd, *J* = 6.9, 1.2 Hz, 5H), 7.31–7.29 (m, 2H), 7.10 (d, *J* = 2.5 Hz, 1H), 2.34 (s, 3H, CH<sub>3</sub> of Ar), 2.29 (s, 6H, CH<sub>3</sub> of Ar), 1.99 (s, 6H, CH<sub>3</sub> of Ar), 1.26 (s, 9H, CH<sub>3</sub> of <sup>t</sup>Bu), 1.21 (s, 9H, CH<sub>3</sub> of <sup>t</sup>Bu). <sup>13</sup>C NMR (101 MHz, CDCl<sub>3</sub>, 25 °C): δ 161.1, 157.5, 155.1, 149.7, 143.2, 141.3, 138.4 (CH), 138.0 (CH), 136.6 (CH), 135.3, 135.1, 133.7, 133.2, 133.0, 130.0, 129.6, 129.2 (CH), 127.7 (CH), 126.5 (CH), 125.1 (fH), 122.6, 122.0, 121.4 (CH), 119.6, 118.4 (CH), 34.4 (C(CH<sub>3</sub>)<sub>3</sub> of <sup>t</sup>Bu), 34.3 (C(CH<sub>3</sub>)<sub>3</sub> of <sup>t</sup>Bu), 31.7 (CH<sub>3</sub> of <sup>t</sup>Bu), 31.6 (CH<sub>3</sub> of <sup>t</sup>Bu), 18.2 (CH<sub>3</sub> of Ar), 17.0 (CH<sub>3</sub> of Ar), 16.9 (CH<sub>3</sub> of Ar).

**Preparation of pyZr<sub>1</sub><sup>ArSiPh<sub>3</sub></sup>.** pyH<sub>2</sub><sup>ArSiPh<sub>3</sub></sup> (100 mg, 0.128 mmol) in benzene (3 mL) was slowly added to a solution of ZrBn<sub>4</sub> (58.2 mg, 0.128 mmol) in benzene (2 mL) under dark conditions. The resulting solution was stirred for 5 h at room temperature. All volatiles were removed under vacuum to give a yellow powder (quantitative yield). <sup>1</sup>H NMR (400 MHz, C<sub>6</sub>D<sub>6</sub>, 25 °C): δ 7.96–7.90 (m, 6H, CH of SiPh<sub>3</sub>), 7.64 (d, *J* = 2.5 Hz, 1H, a phenol ring), 7.52 (d, *J* = 2.5 Hz, 1H, a phenol ring), 7.38–7.35 (m, 2H, CH of py and a phenol ring), 7.28–7.25 (m, 2H, CH of py and a phenol ring), 7.22–7.19 (m, 9H, CH of SiPh<sub>3</sub>), 7.00 (t, *J* = 7.9 Hz, 1H, CH of py), 6.70–6.64 (m, 2H, CH of Bn), 6.61 (t, *J* = 7.3 Hz, 4H, CH of Bn), 6.11 (d, *J* = 6.4 Hz, 4H, CH of Bn), 2.23 (s, 3H, CH<sub>3</sub> of Ar), 2.21 (s, 6H, CH<sub>3</sub> of Ar), 2.18 (s, 6H, CH<sub>3</sub> of Ar), 1.82 (d, *J* = 8.5 Hz, 2H, CH<sub>2</sub> of Bn), 1.32 (s, 9H, CH<sub>3</sub> of <sup>t</sup>Bu), 1.23 (s, 9H, CH<sub>3</sub> of <sup>t</sup>Bu), 0.96 (d, *J* = 8.3 Hz, 2H, CH<sub>2</sub> of Bn). <sup>13</sup>C NMR (101 MHz, C<sub>6</sub>D<sub>6</sub>, 25 °C): δ 161.3, 160.8, 160.4, 152.7, 142.2, 142.1, 140.6 (CH of py), 139.7 (CH of a phenol ring), 137.2, 137.1, 137.0 (CH of a phenyl ring), 135.8, 133.9, 132.5<sub>0</sub>, 132.4<sub>8</sub> (CH of a phenol ring), 132.3, 131.4, 131.2, 130.0 (CH), 129.8 (CH of Bn), 129.5 (CH of Bn), 128.6 (CH of a phenyl ring), 127.1, 127.1, 126.7 (CH), 124.2 (CH), 124.1 (CH), 122.7 (CH of Bn), 122.0, 58.2 (CH<sub>2</sub> of Bn), 34.4 (C(CH<sub>3</sub>)<sub>3</sub> of <sup>t</sup>Bu), 31.8 (CH<sub>3</sub> of <sup>t</sup>Bu), 31.6 (CH<sub>3</sub> of <sup>t</sup>Bu), 18.9 (CH<sub>3</sub> of Ar), 16.9 (CH<sub>3</sub> of Ar), 16.8 (CH<sub>3</sub> of Ar). Anal. Calcd for C<sub>68</sub>H<sub>69</sub>NO<sub>2</sub>SiZr: C, 77.67; H, 6.61; N, 1.33. Found: C, 77.29; H, 6.66; N, 1.44.

**General Procedure for 1-Hexene Polymerization.** In the glovebox, a Schlenk tube was charged with a stirbar, 1-hexene (2.5 mL, 20.0 mmol, 5000 equiv), 1.5 mL of PhCl, and Zr catalyst (4.0 μmol, 1 equiv) in 0.5 mL of PhCl. [CPh<sub>3</sub>][B(C<sub>6</sub>F<sub>5</sub>)<sub>4</sub>] (3.7 mg, 4.0 μmol) in 0.5 mL of PhCl was added, and the reaction stirred 10 min then quenched by addition of 0.5 mL of MeOH in 5 mL of hexanes. In the case of dried MAO and the anilinium activator, a Schlenk tube was charged with a stirbar, 1-hexene (2.5 mL, 20.0 mmol, 5000 equiv), 2.0 mL of PhCl, and dried MAO (58.0 mg, 1.00 mmol, 250 equiv) or [HNMe<sub>2</sub>Ph][B(C<sub>6</sub>F<sub>5</sub>)<sub>4</sub>] (3.2 mg, 4.0 μmol). Then the Zr catalyst (4.0 μmol, 1 equiv) in 0.5 mL of PhCl was added, and the reaction stirred for 10 min before quenching by addition of 0.5 mL of MeOH in 5 mL of hexanes. (Note: MAO was purchased from Albemarle, and volatiles were removed first at room temperature and then under high vacuum at 110 °C for 12 h.) Volatiles were removed under reduced pressure, and the resulting highly viscous oil was dried in a vacuum oven at 150 °C for 10 h. <sup>13</sup>C{<sup>1</sup>H} NMR were acquired in CDCl<sub>3</sub> on a 500 MHz instrument, and samples were prepared using ca. 50 mg of isolated polymer. Integration of the C<sub>3</sub> signal was used to determine the % *mmmm*, where the region of δ 35.1–34.58 was assigned to the *mmmm* pentad and the region of δ 34.58–33.1 was assigned to the remaining pentads.<sup>17</sup>

**General Procedure for Ethylene and Propylene Homo- and Copolymerizations.** Ethylene and propylene homopolymerizations were carried out in a 250 mL Büchi glass autoclave using an Imtech (The Netherlands) laboratory-scale reactor system. The reactor was heated to 120 °C and was purged several times with Ar to remove air and moisture. It was then cooled to 60 °C under Ar and charged with 85 mL of toluene, 2.5 mL (10.0 mmol, 1000 equiv) of MAO, and 0.01 mmol of Zr catalyst in 2 mL of toluene. The reactor was pressurized to 5 bar with ethylene or propylene and maintained at that pressure for 1 h. For ethylene–propylene copolymerizations the pressure was maintained at 5 bar using an ethylene–propylene feed with a 2:3 flow ratio. Gas consumption was measured by a mass flow controller (Brooks Instrument). After 1 h the reactor was degassed and quenched by addition of 30 mL of 5% HCl–MeOH. The polymer was isolated by filtration, washed with fresh methanol, and dried under high vacuum.

**General Procedure for the Copolymerization of Ethylene with 1-Hexene and 1-Tetradecene.** The polymerizations were carried out in a 250 mL Büchi glass autoclave using an Imtech (The Netherlands) laboratory-scale reactor system. The reactor was prepared in the same manner as for homopolymerizations; however, it was charged with 65 mL of toluene, 20 mL of comonomer, 2.5 mL of MAO (10.0 mmol, 1000 equiv), and 0.01 mmol of Zr catalyst in 2 mL of toluene and run at 3 bar of ethylene pressure.

**GPC Analysis.** Gel permeation chromatographic analyses of ethylene and propylene homo- and copolymers were performed at 160 °C using a PL-GPC 220 (Agilent Technologies) equipped with two PLgel Olexis 300 × 7.5 mm columns. BHT (0.0125 wt %) was added to 1,2,4-trichlorobenzene to prevent polymer sample degradation. A sample solution of 5 mg/1.5 mL (*w/v*) was prepared at 140 °C in the prepared solvent, and 100 μL was injected into the GPC columns. Chromatogram data were analyzed using the Cirrus software, which was calibrated using polystyrene standards. The polystyrene-based calibration curve was converted into the universal one using the Mark–Houwink constants of polystyrene (*K* = 0.000 121 dL/g and *α* = 0.707) and polyethylene (*K* = 0.000 406 dL/g and *α* = 0.725).<sup>17</sup>

**Differential Scanning Calorimetry Analysis.** Differential scanning calorimetric (DSC) analysis was performed using a DSC Q2000 (TA Instruments). The temperature and heat flow of the apparatus were calibrated with an indium standard. Polymer samples were first equilibrated at 25 °C, followed by heating from 25 to 200 °C at a rate of 10 °C/min under N<sub>2</sub> flow (5 mL/min). This temperature was maintained for 5 min. Then samples were cooled to 25 °C at a rate of 10 °C/min. This temperature was maintained for 5 min; then samples were reheated to 200 °C at a rate of 10 °C/min. The melting temperature (*T<sub>m</sub>*) was determined from the second heating scan. The percent crystallinity was calculated from Δ*H<sub>f</sub>*(J/g)/Δ*H<sub>std</sub>*(J/g), where

$\Delta H_{\text{std}}$  is the heat of fusion for a perfectly crystalline polyethylene; this is equal to 290.0 J/g.<sup>18</sup>

**Polymer NMR Characterization.** NMR spectra of ethylene- $\alpha$ -olefin copolymers and propylene homopolymers were acquired in  $\text{C}_2\text{D}_2\text{Cl}_4$  on a Varian Inova 500 at 130 °C following a 10 min temperature equilibration period.  $^{13}\text{C}\{^1\text{H}\}$  NMR spectra were integrated, and the percent incorporation was calculated based on literature assignments.<sup>19,20</sup>

## ■ ASSOCIATED CONTENT

### ● Supporting Information

The Supporting Information is available free of charge on the ACS Publications website at DOI: 10.1021/acs.organo- met.7b00015.

Detailed experimental procedures for ligand precursors, full polymerization tables, and spectroscopic data (PDF) X-ray crystallographic data for compounds  $\text{Zr}_1^{\text{ArSiPr}_3}$ - $\text{NMe}_2$ ,  $\text{Zr}_2^{\text{SiPr}_3}$ - $\text{NMe}_2$ , and  $\text{anthZr}_2^{\text{SiPr}_3}$ - $\text{NMe}_2$  (CIF)

## ■ AUTHOR INFORMATION

### Corresponding Author

\*E-mail: agapie@caltech.edu.

### ORCID

Theodor Agapie: 0000-0002-9692-7614

### Notes

The authors declare no competing financial interest.

## ■ ACKNOWLEDGMENTS

Mike Takase, Larry Henling, and Heui Beom Lee are acknowledged for crystallographic assistance. We thank Prof. Grubbs for allowing access to a GPC instrument in his laboratory at Caltech for measurements of 1-hexene homopolymers. The authors are grateful for the support provided by King Fahd University of Petroleum and Minerals, Dhahran, Saudi Arabia, offered under the KFUPM-Caltech Research Collaboration.

## ■ REFERENCES

- (1) Delferro, M.; Marks, T. J. *Chem. Rev.* **2011**, *111*, 2450–2485.
- (2) Li, L.; Metz, M. V.; Li, H.; Chen, M.-C.; Marks, T. J.; Liable-Sands, L.; Rheingold, A. L. *J. Am. Chem. Soc.* **2002**, *124*, 12725–12741.
- (3) Salata, M. R.; Marks, T. J. *J. Am. Chem. Soc.* **2008**, *130*, 12–13.
- (4) Gao, Y.; Mouat, A. R.; Motta, A.; Macchioni, A.; Zuccaccia, C.; Delferro, M.; Marks, T. J. *ACS Catal.* **2015**, *5*, 5272–5282.
- (5) Takeuchi, D.; Chiba, Y.; Takano, S.; Osakada, K. *Angew. Chem., Int. Ed.* **2013**, *52*, 12536–12540.
- (6) (a) Takano, S.; Takeuchi, D.; Osakada, K.; Akamatsu, N.; Shishido, A. *Angew. Chem., Int. Ed.* **2014**, *53*, 9246–9250. (b) Takano, S.; Takeuchi, D.; Osakada, K. *Chem. - Eur. J.* **2015**, *21*, 16209–16218.
- (7) (a) Radlauer, M.; Day, M. W.; Agapie, T. *Organometallics* **2012**, *31*, 2231–2243. (b) Radlauer, M. R.; Day, M. W.; Agapie, T. *J. Am. Chem. Soc.* **2012**, *134*, 1478–1481. (c) Radlauer, M. R.; Buckley, A. K.; Henling, L. M.; Agapie, T. *J. Am. Chem. Soc.* **2013**, *135*, 3784–3787.
- (8) (a) Coates, G. W. *Chem. Rev.* **2000**, *100*, 1223–1252. (b) Brintzinger, H. H.; Fischer, D.; Mühlaupt, R.; Rieger, B.; Waymouth, R. M. *Angew. Chem., Int. Ed. Engl.* **1995**, *34*, 1143–1170.
- (9) (a) Gibson, V. C.; Spitzmesser, S. K. *Chem. Rev.* **2003**, *103*, 283–315. (b) Britovsek, G. J. P.; Gibson, V. C.; Wass, D. F. *Angew. Chem., Int. Ed.* **1999**, *38*, 428–447. (c) Resconi, L.; Cavallo, L.; Fait, A.; Piemontesi, F. *Chem. Rev.* **2000**, *100*, 1253–1346.
- (10) Wei, J.; Hwang, W.; Zhang, W.; Sita, L. R. *J. Am. Chem. Soc.* **2013**, *135*, 2132–2135.
- (11) (a) Lee, D.-H.; Yoon, K.-B.; Lee, E.-H.; Noh, S.-K.; Byun, G.-G.; Lee, C.-S. *Macromol. Rapid Commun.* **1995**, *16*, 265–268. (b) Noh, S. K.; Byun, G.-G.; Lee, C.-S.; Lee, D.; Yoon, K.-B.; Kang, K. S. J.

*Organomet. Chem.* **1996**, *518*, 1–6. (c) Noh, S. K.; Kim, S.; Yang, Y.; Lyoo, W. S.; Lee, D.-H. *Eur. Polym. J.* **2004**, *40*, 227–235. (d) Noh, S. K.; Jung, W.; Oh, H.; Lee, Y. R.; Lyoo, W. S. *J. Organomet. Chem.* **2006**, *691*, 5000–5006. (e) Linh, N. T. B.; Huyen, N. T. D.; Noh, S. K.; Lyoo, W. S.; Lee, D.-H.; Kim, Y. *J. Organomet. Chem.* **2009**, *694*, 3438–3443.

(12) Radlauer, M. R.; Agapie, T. *Organometallics* **2014**, *33*, 3247–3250.

(13) (a) Groysman, S.; Tshuva, E. Y.; Reshef, D.; Gendler, S.; Goldberg, I.; Kol, M.; Goldschmidt, Z.; Shuster, M.; Lidor, G. *Isr. J. Chem.* **2002**, *42*, 373–381. (b) Tshuva, E. Y.; Groysman, S.; Goldberg, I.; Kol, M.; Goldschmidt, Z. *Organometallics* **2002**, *21*, 662–670. (c) Tshuva, E. Y.; Goldberg, I.; Kol, M.; Weitman, H.; Goldschmidt, Z. *Chem. Commun.* **2000**, 379–380. (d) Tshuva, E. Y.; Goldberg, I.; Kol, M.; Goldschmidt, Z. *Organometallics* **2001**, *20*, 3017–3028. (e) Groysman, S.; Goldberg, I.; Kol, M.; Genizi, E.; Goldschmidt, Z. *Inorg. Chim. Acta* **2003**, *345*, 137–144. (f) Groysman, S.; Goldberg, I.; Kol, M.; Genizi, E.; Goldschmidt, Z. *Organometallics* **2003**, *22*, 3013–3015. (g) Switzer, J. M.; Travia, N. E.; Steelman, D. K.; Medvedev, G. A.; Thomson, K. T.; Delgass, W. N.; Abu-Omar, M. M.; Caruthers, J. M. *Macromolecules* **2012**, *45*, 4978–4988. (h) Steelman, D. K.; Xiong, S.; Pletcher, P. D.; Smith, E.; Switzer, J. M.; Medvedev, G. A.; Delgass, W. N.; Caruthers, J. M.; Abu-Omar, M. M. *J. Am. Chem. Soc.* **2013**, *135*, 6280–6288. (i) Steelman, D. K.; Pletcher, P. D.; Switzer, J. M.; Xiong, S.; Medvedev, G. A.; Delgass, W. N.; Caruthers, J. M.; Abu-Omar, M. M. *Organometallics* **2013**, *32*, 4862–4867. (j) Steelman, D. K.; Xiong, S.; Medvedev, G. A.; Delgass, W. N.; Caruthers, J. M.; Abu-Omar, M. M. *ACS Catal.* **2014**, *4*, 2186–2190. (k) Pletcher, P. D.; Switzer, J. M.; Steelman, D. K.; Medvedev, G. A.; Delgass, W. N.; Caruthers, J. M.; Abu-Omar, M. M. *ACS Catal.* **2016**, *6*, 5138–5145. (l) Reybuck, S. E.; Lincoln, A. L.; Ma, S.; Waymouth, R. M. *Macromolecules* **2005**, *38*, 2552–2558.

(14) (a) Busico, V.; Cipullo, R.; Ronca, S.; Budzelaar, P. H. M. *Macromol. Rapid Commun.* **2001**, *22*, 1405–1410. (b) Cohen, A.; Kopilov, J.; Goldberg, I.; Kol, M. *Organometallics* **2009**, *28*, 1391–1405. (c) Gendler, S.; Zelikoff, A. L.; Kopilov, J.; Goldberg, I.; Kol, M. *J. Am. Chem. Soc.* **2008**, *130*, 2144–5. (d) Segal, S.; Goldberg, I.; Kol, M. *Organometallics* **2005**, *24*, 200–202.

(15) (a) Golisz, S. R.; Bercaw, J. E. *Macromolecules* **2009**, *42*, 8751–8762. (b) Agapie, T.; Henling, L. M.; DiPasquale, A. G.; Rheingold, A. L.; Bercaw, J. E. *Organometallics* **2008**, *27*, 6245–6256. (c) Kirillov, E.; Roisnel, T.; Razavi, A.; Carpentier, J.-F. *Organometallics* **2009**, *28*, 5036–5051.

(16) Pangborn, A. B.; Giardello, M. A.; Grubbs, R. H.; Rosen, R. K.; Timmers, F. J. *Organometallics* **1996**, *15*, 1518–1520.

(17) Atiqullah, M.; Moman, A. A.; Akhtar, M. N.; Al-Muallem, H. A.; Abu-Raqabah, A. H.; Ahmed, N. *J. Appl. Polym. Sci.* **2007**, *106*, 3149–3157.

(18) Dias, P.; Lin, Y. J.; Poon, B.; Chen, H. Y.; Hiltner, A.; Baer, E. *Polymer* **2008**, *49*, 2937–2946.

(19) (a) Carman, C. J.; Harrington, R. A.; Wilkes, C. E. *Macromolecules* **1977**, *10*, 536–544. (b) Cheng, H. N. *Macromolecules* **1984**, *17*, 1950–1955. (c) Cheng, H. N.; Smith, D. A. *Macromolecules* **1986**, *19*, 2065–2072. (d) Randall, J. C. *Macromolecules* **1978**, *11*, 33–36. (e) Randall, J. C.; Hsieh, E. T. *Macromolecules* **1982**, *15*, 1584–1586. (f) Tritto, I.; Fan, Z.-Q.; Locatelli, P.; Sacchi, M. C.; Camurati, I.; Galimberti, M. *Macromolecules* **1995**, *28*, 3342–3350.

(20) (a) Hsieh, E. T.; Randall, J. C. *Macromolecules* **1982**, *15*, 1402–1406. (b) Cheng, H. N. *Polym. Bull.* **1991**, *26*, 325–332. (c) Galland, G. B.; Mauler, R. S.; de Menezes, S. C.; Quijada, R. *Polym. Bull.* **1995**, *34*, 599–604. (d) Quijada, R.; Dupont, J.; Miranda, M. S. L.; Scipioni, R. B.; Galland, G. B. *Macromol. Chem. Phys.* **1995**, *196*, 3991–4000.

(21) Yeori, A.; Goldberg, I.; Shuster, M.; Kol, M. *J. Am. Chem. Soc.* **2006**, *128*, 13062–13063.

(22) Sworen, J. C.; Smith, J. A.; Wagener, K. B.; Baugh, L. S.; Rucker, S. P. *J. Am. Chem. Soc.* **2003**, *125*, 2228–2240.